İSTANBUL TECHNICAL UNIVERSITY ★ INSTITUTE OF SCIENCE AND TECHNOLOGY

STATIC AND DYNAMIC ANALYSES OF PLATES USING DIFFERENTIAL QUADRATURE METHOD (DQM)

M.Sc. Thesis by
Murat Tuna

Department :   Aeronautics and Astronautics Engineering

Programme :   Aeronautics and Astronautics Engineering

June 2009

İSTANBUL TECHNICAL UNIVERSITY ★ INSTITUTE OF SCIENCE AND TECHNOLOGY

STATIC AND DYNAMIC ANALYSES OF PLATES USING DIFFERENTIAL QUADRATURE METHOD (DQM)

M.Sc. Thesis by
Murat Tuna
(511061020)

Date of submission :	**May 04, 2009**
Date of defence examination:	**June 04, 2009**

Supervisor (Chairman) :	**Assoc. Prof. Dr. Halit S. Türkmen (ITU)**
Members of the Examining Committee :	**Prof. Dr. Zahit Mecitoğlu (ITU)**
	Assoc. Prof. Dr. Ekrem Tüfekçi (ITU)

June 2009

İSTANBUL TEKNİK ÜNİVERSİTESİ ★ FEN BİLİMLERİ ENSTİTÜSÜ

DİFERANSİYEL KARELEME YÖNTEMİ İLE PLAKLARIN STATİK VE DİNAMİK ANALİZİ

YÜKSEK LİSANS TEZİ
Murat Tuna
(511061020)

Tezin Enstitüye Verildiği Tarih :   04 Mayıs 2009
Tezin Savunulduğu Tarih :   04 Haziran 2009

Tez Danışmanı :   Doç. Dr. Halit S. Türkmen (İTÜ)
Diğer Jüri Üyeleri :   Prof. Dr. Zahit Mecitoğlu (İTÜ)
Doç. Dr. Ekrem Tüfekçi (İTÜ)

Haziran 2009

FOREWORD

I would like to express my appreciations to Assoc. Prof. Dr. Halit S. Türkmen for his guidance and advice throughout this study. I am especially thankful for the analyses he achieved which made this work meaningful. The author is also grateful to Prof. Dr. Zahit Mecitoğlu and Assoc. Prof. Dr. Ekrem Tüfekçi for their valuable comments.

July 2009   Murat Tuna

                                                          Aeronautical Engineer

TABLE OF CONTENTS

LIST OF TABLES

LIST OF FIGURES

STATIC AND DYNAMIC ANALYSES OF PLATES USING DIFFERENTIAL QUADRATURE METHOD

SUMMARY

In this study, static and dynamic analyses of isotropic and layered composite square plates have been achieved using differential quadrature method (DQM). Differential quadrature method is a highly efficient and a newly proposed numerical technique compared to the conventional ones like finite element, finite difference and etc. Using this method, isotropic and laminated composite thin plates are analyzed from various aspects such as plate material and thickness. Two types of boundary condition are analyzed: Simply supported and clamped on all four edges. For the plate material, various isotropic and laminated composites are considered. Plates of variable thickness are also analyzed.

In the first analysis section, deflection analysis has been achieved for the isotropic and composite laminated plates of constant and varying thickness. After deriving the analytical governing equations, the DQM analogue equations are obtained. In the further sections, the mentioned way also followed for the free vibration and transient analyses of aforementioned plates. In the section of transient analyses, plates are assumed to be exposed to blast loading and the resulting DQM equations are solved using Newmark time integration method. After all governing DQM analogue equations are derived in the mentioned sections, the numerical results obtained by using these equations are presented. Then, the obtained DQM results are compared to mainly ANSYS results, and for some plate configurations, compared to experimental, theoretical and some DQM results from the literature.

From the results presented in the relevant section, it can be concluded that DQM provides result with adequate accuracy for the static, free vibrational and transient analyses of both isotropic and laminated composite plates. Moreover, it is observed that DQM can also be applied to tapered plates, successfully. Furthermore, the formulation of DQM solutions is simple and the computer programming procedure is also considerably straightforward. The computation time is also significantly less than the finite element method. Consequently, DQM seems to have the potential to be an alternative to the conventional numerical techniques like finite element and finite difference.

DİFERANSİYEL KARELEME YÖNTEMİ İLE PLAKLARIN STATİK VE DİNAMİK ANALAZİ

ÖZET

Bu tezde, izotropik ve katmanlı kompozit ince kare plakların diferansiyel kareleme (DKY) yöntemi ile statik ve dinamik analizleri gerçekleştirilmiştir. Plaklar, çeşitli izotopik ve kompozit malzemeler kullanılarak bütün kenarlarından ankastre ya da basit mesnetli olmak üzere iki farklı sınır koşulu için incelenmiştir. Ayrıca, plaklar kalınlıkları açısından da analiz edilmiştir. Sabit kalınlıklı plaklarla beraber x-ekseni yönünde kalınlığı lineer değişen izotropik ve katmanlı kompozit ince kare plaklar analizlerde kullanılmıştır.

Tezin, ilk analiz bölümünde sözü edilen basit ve ankastre plakların çökme analizleri DKY kullanılarak gerçekleştirilmiştir. Sonraki bölümde ise, plakların serbest titreşim frekanslarını veren yönetici denklemler çıkarılmış ve çözümde kullanılmak üzere, DKY'ne göre benzeşim denklemleri yazılmıştır. Aynı süreç, plakların geçişli analizlerinin yapıldığı son analiz bölümünde de tekrarlanmıştır. Geçişli analizlerde, plakların, anlık basınç yüküne maruz olduğu kabulü yapılmış ve ilgili denklemler Newmark sayısal integrasyon yöntemi kullanılarak çözülmüştür. Sayısal sonuçların verildiği bölümde öncelikle plaklar için kullanılan izotropik ve kompozit malzemelerin özellikleri verilmiştir. Daha sonrasında ise, her bir plak yapılandırması için elde edilen DKY denklemlerinin çözümü vasıtasıyla elde edilen sayısal sonuçlar verilmiştir. Sonuçlar, her aşamada ANSYS yazılımı sonuçları ile ve aynı zamanda bazı plaklar için literatürde bulunan bazı deneysel, teorik ve sayısal yöntem sonuçları ile karşılaştırılmıştır.

Elde edilen sayısal sonuçlara dayanılarak denilebilir ki, diferansiyel kareleme yöntemi ile izotropik ve kompozit plakların statik, dinamik ve geçişli analizleri başarıyla gerçekleştirilebilir. Aynı zamanda, yöntemin, değişken kalınlıklı plakların analizine de başarıyla uygulanabildiği görülmüştür. DKY kullanılarak sonuçların bilgisayarda elde edilme süresi, sonlu elemanlar yöntemine göre oldukça düşük olduğu da gözlenmiştir. Programlaması basit ve az işlem yükü ile yeterli hassasiyette doğru sonuçlar veren diferansiyel kareleme yöntemi, mühendislikte ve bilimde yoğun olarak kullanılan sonlu farklar ve sonlu elemanlar gibi yöntemlere alternatif olarak gösterilebilir.

1. INTRODUCTION

In this study, static, free vibration and transient analyses of isotropic and layered composite rectangular plates have been achieved using differential quadrature method (DQM). After verifying the accuracy of the DQM solutions by obtaining deflections and free vibration frequencies of isotropic and laminated composite plates and comparing with other results, structural response of isotropic and laminated composite plates subjected to air blast loading obtained by DQM and compared to ANSYS results and some other available results in literature. That is to say, this work mostly based on obtaining the structural response of plates subjected to air blast load by DQM and verifying the accuracy of obtained results. As it will be noted in the further sections, various plate configurations such as isotropic and composite plates of constant and variable thickness are investigated by DQM.

Plates subjected to air blast load have been investigated by different researchers widely. For example, Turkmen and Mecitoğlu investigated nonlinear structural response of laminated composite plates subjected to air blast load [1]. In the present work some of the DQM results were compared to the theoretical and experimental results given in the mentioned paper.

Differential quadrature method is a highly efficient and a newly proposed numerical technique compared to the conventional ones like finite element, finite difference and etc. It has been introduced in 1970s by R. Bellman and his associates for rapid and more accurate solution of linear and nonlinear partial differential equations [2, 3]. In the following years of 1970s, the method has been improved more by different researchers and has been applied to many different engineering problems successfully. For instance, it has been applied to the transport processes and multi-dimensional problems by Civan and Sliepcevich [4,5] and to the nonlinear diffusion by Mingle [6]. It was the first time when Bert and et al. used the method to solve a problem from structural mechanics which involves fourth-order partial differential equation [7]. Following this, Jang and et al. applied the method to the static analysis of structural components; Wang and et al. applied to the problems of deflection,

buckling and free vibration of beams and plates; Malik and Bert applied to the problem of free vibration of plates in a new respect, and Shu et al. applied to Navier-Stokes equations. [8-13]. It also should be stated that the analytical results given in the paper of Leisa [14] are used as reference for the obtained DQM results.

Not only simple thin plates, but also the plates involve some complicating effects like thickness non-uniformity, material anisotropy, have been analyzed using DQM. For instance, The Bert et al. solved free vibration problem of symmetrically laminated cross-ply plates based on the first-order shear deformable plate theory using DQM [15]. Turkmen investigated structural response of isotropic plates subjected to air blast load comparing the theoretical and experimental results [16]. Farsa et al. obtained fundamental frequency of isotropic tapered plates [17]; Farsa [18] and Farsa et al. [19] achieved fundamental frequency analysis of single specially orthotropic, generally orthotropic and anisotropic rectangular layered plates by the differential quadrature method. Tuna and Turkmen, used DQM to obtain structural response of plates subjected to air blast load [20, 21]. Furthermore, Bert and et al. accomplished static and free vibration analyses of isotropic and anisotropic plates by DQM [22, 23]. Moreover, Bert and Malik utilized the DQM for irregular domains and applied to plate vibration in another work [24] and also developed a semi-analytical differential quadrature solution for plate problems in a few works [25, 26]. The papers referenced so far demonstrate that DQM is an efficient numerical technique and capable of yielding results of high accuracy in computational mechanics. It has been applied successfully to many problems in structural mechanics by investigators. However, as stated by Bert and Malik [10], DQM is still in a developing stage and the problems that the DQM applied to so far, have been limited to smaller scale ones. Consequently, overcoming the limitations of applying DQM to other type of problems or large scale problems offers challenges to future DQM researchers.

As stated earlier, present work based mostly on obtaining the structural response of plates subjected to blast loading by DQM. Blast loaded plates have also been investigated by researchers formerly. For instance, as mentioned earlier, Turkmen and Mecitoglu have also obtained nonlinear structural response of laminated composite plates subjected to blast loading [1], and Turkmen investigated structural response of isotropic plates subjected to blast loading [16]. In these studies,

experimental results are compared with theoretical method and FEM results by the authors. Furthermore, Kazanci and Mecitoglu investigated the nonlinear damped vibrations of composite plates subject to blast loading [27].

In this work, static, free vibration and transient analyses of plates are achieved using DQM. Only, simply supported and clamped plates on all four edges are considered. Various isotropic and laminated composite materials are employed in the analyses. However, plates of linearly variable thickness are also analyzed using DQM in each analyse section. For the each plate configuration, static, free vibration and transient analyses are accomplished in the relevant sections. Before going into detail of analyses, some basic definitions of DQM are given in the Section 2. In this section, formulas relevant to obtaining the weighting coefficients of DQM and some discussions related with incorporation of the boundary conditions into the DQM solutions are introduced after the mathematical basis of the method is presented.

In the Section 3, deflection analysis has been achieved for the isotropic and laminated composite plates of constant and variable thickness. After deriving the analytical governing equations, the DQM analogue equations are obtained from which the deflections are obtained. In the fourth section, free vibration analyses are accomplished by DQM for the mentioned plates. After presenting of the governing free vibration equations (eigenvalue equations) for each plate configuration, the DQM analogue equations are derived. Once the DQM governing equations are derived, the free vibration frequencies can be obtained for each mode.

The transient analyses of aforementioned plates are presented in the Section 5. In this section, plates are assumed to be exposed to blast loading. Following the same way again, the governing analytical equations are presented for each plate configuration firstly. And then, DQM analogue equations are derived to be solved. However, it is worth to express that the solutions of the governing equations in this section involves using time integration tool differently from the previous sections. Therefore, the obtained DQM equations are solved here using a time integration method. In this work, the Newmark time integration method is employed in the solutions.

Numerical results are presented in the Section 6. In this section, numerical results for the plates of constant thickness are given firstly. In the second subsection the numerical results for plates of variable thickness are given. Before presenting the numerical results, the material properties that used in the analyses are given. As it

will be noticed in this section, some results are given dimensionless whereas some are given dimensional for convenience. The centre deflections are given firstly in this section for the each plate configuration. The obtained results are tabulated in tables to compare with ANSYS results and some available DQM and theoretical results from the literature. Subsequently, the fundamental free vibration frequencies are presented in tables with ANSYS and available results from the literature for comparison.

The results of transient analyses are given using two different parameters: deflection and strain of plate centres. That is, deflection-time and strain-time histories of plate centres are obtained using DQM and compared to mainly ANSYS results, and for some plate configurations, compared to experimental and theoretical results found in the literature.

Experiences show that DQM is a highly efficient numerical technique for investigating of plates of constant and variable thickness. Plates of laminated composite are also easily analyzed and results with high accuracy can be obtained using DQM. It is especially worth to express that transient analysis of isotropic and composite plates subject to blast load is easily achieved by DQM. The solution time with DQM is quite less than ANSYS solution, and developing of computer programs for DQM solutions is quite simple. This would be a significant advantage through the long-time transient analyses. As it will also be stated in the further section, once the weighting coefficients in DQM solutions are obtained, they might be used in every kind of problem regardless of problem type or boundary conditions which is an efficient side of DQM.

2. DIFFERENTIAL QUADRATURE METHOD (DQM)

In this section, the differential quadrature method (DQM) is described briefly. Firstly, the mathematical definition of DQM is presented and some significant differences from other conventional numerical techniques are explained. Later, a tool to obtain the weighting coefficients to be used in DQM solutions is explained and the relevant formulas are given. Lastly, some discussions about implementation of the boundary conditions in DQM solutions are introduced. Two commonly used approaches for incorporating of boundary condition into DQM solutions among the DQM researchers are illustrated briefly.

2.1 Mathematical Definition of DQM

In DQM, a partial derivative of a function with respect to a coordinate direction is expressed as a linear weighted sum of all the functional values at all mesh points along that direction. In other words, the DQM reduces the differential equations into an analogous set of algebraic equations by expressing at each grid point the calculus operator value of a function with respect to a coordinate direction at any discrete point as the weighted linear sum of the values of the function at all the discrete points chosen in that direction [10].
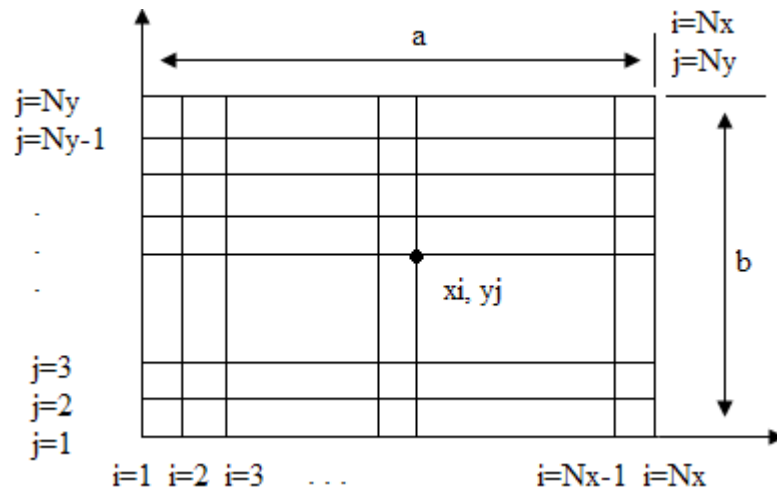
Fig. 2.1 Quadrature grid for a rectangular region

For instance, a function $\psi = \psi(x, y)$ which has a rectangular domain $0 \leq x \leq a$, $0 \leq x \leq b$ like in the Fig. 2.1 can be considered. Assuming that the function values in the solution domain are known or desired on a grid of sampling points, the rth-order partial derivatives of the function $\psi(x, y)$ with respect to x and y at points $x = x_i$ and $y = y_j$ along any lines $y = y_j$ and $x = x_i$ are expressed in terms of the DQM, respectively, as following

$$\left.\frac{\partial^r \psi}{\partial x^r}\right|_{x=x_i} = \sum_{k=1}^{N_x} A_{ik}^{(r)} \psi_{kj}, \qquad i = 1,2,...,N_x \tag{2.1a}$$

$$\left.\frac{\partial^r \psi}{\partial y^r}\right|_{y=y_i} = \sum_{l=1}^{N_y} B_{jl}^{(r)} \psi_{il}, \qquad j = 1,2,...,N_y \tag{2.1b}$$

Above, $A_{ik}^{(r)}$ and $B_{jl}^{(r)}$ are the weighting coefficients of rth order x and y derivatives, N_x and N_y are the number of grid points taken in the x and y directions in the domain, respectively.

The method of differential quadrature uses a polynomial fitting at the selected points. This is one of major differences of this method compared to other numerical methods such as (higher order) finite difference which is mainly a Taylor expansion based method. Another difference is that in the standard finite difference method a solution value at a point is expressed as a function of the values at adjacent points only whereas differential quadrature method takes all the function values at all the discrete points in the domain. The finite element method, however, is based on weighted residuals and provides a better approximation for irregular shaped systems compared to the finite difference method. The shared principle of these methods is that both of them have the discretization principle and divide the solution domain into many simply shaped regions. Thus, solutions obtained by these methods have to be computed using a large number of surrounding points to be able obtain a solution with a high accuracy since the accuracy strongly depends on the nature and refinement of the discretization of the domain. However, at most time, the differential quadrature method provides solutions with high accuracy using only few number of grid points compared to abovementioned methods. The computer programming system of DQM solutions is also straightforward which provides a significant efficiency through the solutions. Therefore DQM has the potential of

being an alternative to the conventional numerical techniques such as the finite difference and finite element methods [10].

2.2 Calculation of Weighting Coefficients

One of the key points of DQM is to determine the weighting coefficients for a discretization of a derivative of any order for the related domain. The weighting coefficients are independent of the boundary conditions and therefore, need to be calculated only once for a particular discretization. The method proposed by Shu and Richards [13] in order to calculate the weighting coefficients, which has also been utilized at the present work, provides solutions with adequate accuracy. The relevant formulas developed by the mentioned method to calculate the weighting coefficients given in the work of Bert and Malik [10] are also given here. Following formula may be used to calculate the weighting coefficients of first-order derivatives

$$A_{ik}^{(1)} = \frac{\prod\limits_{\upsilon=1,\upsilon\neq i}^{Nx} (x_i - x_\upsilon)}{(x_i - x_k) \prod\limits_{\upsilon=1,\upsilon\neq k}^{Ny} (x_k - x_\upsilon)} \quad \text{for } i,\, k = 1,2,\ldots,N_x \text{ and } i \neq k \tag{2.2}$$

The terms of weighting coefficients matrix of second- and higher-order derivatives may be obtained through the following relationship

$$A_{ik}^{(r)} = r\left[A_{ii}^{(r-1)} A_{ik}^{(1)} - \frac{A_{ik}^{(r-1)}}{x_i - x_k} \right] \quad \text{for } i,k = 1,2,\ldots,N_x \text{ and } k \neq i \tag{2.3}$$

where $2 \leq r \leq (N_x - 1)$. The diagonal terms of the weighting coefficient matrix are given by

$$A_{ii}^{(r)} = -\sum_{\upsilon=1,\upsilon\neq i}^{N_x} A_{i\upsilon}^{(r)} \quad \text{for } i = 1,2,\ldots,N_x \tag{2.4}$$

where $1 \leq r \leq (N_x - 1)$. Following equation to calculate the coordinates of the sampling points is used in the present study

$$x_i = \frac{1 - \cos[(i-1)\pi/(N_x - 1)]}{2} a; \qquad i = 1,2,\ldots,N_x \tag{2.5}$$

7

One may see the work of Bert and Malik [10] for other types of calculating the coordinates of sampling points and other regarding matters.

2.3 Implementation of Boundary Conditions

Currently, there are two approaches are popular among DQM researchers for implementation boundary conditions. Here, both approaches will be explained briefly. Some references relevant to the topic will also be given for the interested readers.

The first approach, which is also most widely used, has a general applicability in many types of problems. This approach based on discretization of governing equation on the grid points of domain and boundary conditions on the boundary grid points, and finally assembling all of them to be solved.

Explaining the mentioned approaches on a one-dimensional problem may be more convenient. Assume a freely vibrating Bernoulli-Euler beam which would has quite general boundary conditions at both ends like simply supported, clamped or free end, but let assume the beam simply supported at both edges for convenience. This example will be a modified form of the one given in the work of Bert and Malik [10] in which a freely vibrating cantilever Bernoulli-Euler beam analyzed by DQM in detail. The linear free vibration of a thin prismatic Bernoulli-Euler beam is described by the following eigenvalue differential equation

$$\frac{d^4 w}{d\xi^4} = \Omega^2 w \qquad\qquad (2.6)$$

where $w = w(\xi)$ is the dimensionless mode function of the lateral deflection, ξ is the dimensionless coordinate along axis of the beam, $\xi = x/L$, and Ω is the dimensionless frequency of the beam vibrations, $\Omega^2 = \bar{m} L^4 \omega^2 / EI$. Here, $\bar{m}$ is the mass per unit length of the beam, L is the length of beam, ω is the dimensional frequency, and E and I are the modulus of elasticity and moment of inertia of the beam, respectively. The boundary conditions at both clamped ends are

$$w = d^2 w / d\xi^2 = 0 \text{ at } \xi = 0 = 1 \qquad\qquad (2.7)$$

As explained in Ref. [10], of the needed N quadrature analogue equations, four equations should be obtained from Eqs. (2.7) for the both ends, and the remaining

(*N-4*) equations from Eq. (2.6). Therefore, leaving two sampling points at each end of beam, quadrature analogue of Eq. (2.6) be written as

$$\sum_{j=1}^{N} A_{ij}^{(4)} w_j = \Omega^2 w_i \ ; \quad i = 3,4,\ldots,(N\text{-}2) \tag{2.8}$$

which yields (*N-4*) equations. The quadrature analogues of the boundary conditions Eqs. (2.7) are written as

$$w_i = 0 \ , \ \sum_{j=1}^{N} A_{ij}^{(2)} w_j = 0 \ ; \ i = 1 \qquad\qquad \text{at } \xi = 0 \tag{2.9.a}$$

$$w_i = 0 \ , \ \sum_{j=1}^{N} A_{ij}^{(2)} w_j = 0 \ ; \ i = N \qquad\qquad \text{at } \xi = 1 \tag{2.9.b}$$

The assembly of Eqs. (2.8) through (2.9) gives following set of linear equations

$$\begin{bmatrix} 1 & 0 & 0 & 0 & 0 & \cdots & 0 \\ A_{11}^{(2)} & A_{12}^{(2)} & A_{1(N-1)}^{(2)} & A_{1N}^{(2)} & A_{13}^{(2)} & \cdots & A_{1(N-2)}^{(2)} \\ 0 & 0 & 0 & 0 & 0 & \cdots & 1 \\ A_{N1}^{(2)} & A_{N2}^{(2)} & A_{N(N-1)}^{(2)} & A_{NN}^{(2)} & A_{N3}^{(2)} & \cdots & A_{N(N-2)}^{(2)} \\ A_{31}^{(4)} & A_{32}^{(4)} & A_{3(N-1)}^{(4)} & A_{3N}^{(4)} & A_{33}^{(4)} & \cdots & A_{3(N-2)}^{(4)} \\ A_{41}^{(4)} & A_{42}^{(4)} & A_{4(N-1)}^{(4)} & A_{4N}^{(4)} & A_{43}^{(4)} & \cdots & A_{4(N-2)}^{(4)} \\ \vdots & \vdots & \vdots & \vdots & \vdots & \cdots & \vdots \\ A_{(N-2)1}^{(4)} & A_{(N-2)2}^{(4)} & A_{(N-2)(N-1)}^{(4)} & A_{(N-2)N}^{(4)} & A_{(N-2)3}^{(4)} & \cdots & A_{(N-2)(N-2)}^{(4)} \end{bmatrix} \times$$

$$\begin{Bmatrix} w_1 \\ w_2 \\ w_{(N-1)} \\ w_N \\ w_3 \\ w_4 \\ \vdots \\ w_{(N-2)} \end{Bmatrix} = \Omega^2 \begin{Bmatrix} 0 \\ 0 \\ 0 \\ 0 \\ w_3 \\ w_4 \\ \vdots \\ w_{(N-2)} \end{Bmatrix} \tag{2.10}$$

Equation (2.10) may be written as

$$\begin{bmatrix} [S_{bb}] & [S_{bd}] \\ [S_{db}] & [S_{dd}] \end{bmatrix} \begin{Bmatrix} \{w_b\} \\ \{w_d\} \end{Bmatrix} = \begin{Bmatrix} \{0\} \\ \Omega^2 \{w_d\} \end{Bmatrix} \tag{2.11}$$

9

where subscript *b* indicates the grid points used for writing the quadrature analog of the boundary conditions, *d* indicates the grid points used for writing the quadrature analog of the governing differential equation. Eliminating the column vector $\{w_b\}$, Eq. (2.11) is reduced to following standard eigenvalue problem

$$[S]\{w_d\} - \Omega^2 [I]\{w_d\} = \{0\} \tag{2.12}$$

where $[S] = [S_{dd}] - [S_{db}][S_{bb}]^{-1}[S_{bd}]$ is of order $(N\text{-}4) \times (N\text{-}4)$.

The eigenvalues, which are the frequency squared values, and the eigenvectors $\{w_d\}$ which describes the mode shapes of the freely vibrating beam may both be determined from the $[S]$ matrix. As it may be noted, boundary conditions are incorporated into the solution by writing the quadrature analogs of equations of boundary conditions at the boundary points and quadrature analog of governing equation at the inner domain points. Assembling all of them give a set of linear equations from which the eigenvalues are solved.

The second approach for applying the boundary conditions to the DQM solutions, which is also utilized in the present work, is based on modifying the weighting coefficients matrices during the formulation of problem. Here, the one dimensional problem - freely vibrating beam given earlier is taken as reference and will be employed to explain the second approach. The governing equation and relevant boundary equations were given by Eqs. (2.6) and (2.7), and their quadrature analogs by (2.8) and (2.9). As described in Ref. [8], the boundary conditions will be implemented during the formulation of the problem.

So, we modify the weighting coefficient matrice of second-order derivative since the second boundary equation at the each end is of second-order. To do so, let the original weighting coefficient matrice of second-order derivative being as follows

$$\left[A_{ij}^{(2)} \right] = \begin{bmatrix} A_{11}^{(2)} & A_{12}^{(2)} & \cdots & A_{1N}^{(2)} \\ A_{21}^{(2)} & A_{22}^{(2)} & \cdots & A_{2N}^{(2)} \\ \vdots & \vdots & \cdots & \vdots \\ A_{N1}^{(2)} & A_{N2}^{(2)} & \cdots & A_{NN}^{(2)} \end{bmatrix} \tag{2.13}$$

To implement the boundary conditions $d^2w/d\zeta^2 = 0$ at $\xi = 0$ and $\xi = 1$ we zero the first (1th) and the last (Nth) columns of $\left[A_{ij}^{(2)} \right]$ matrix. So, representing the modified matrix as $\left[\tilde{A}_{ij}^{(2)} \right]$ we obtain

$$
\left[\tilde{A}_{ij}^{(2)} \right] = \begin{bmatrix} 0 & A_{12}^{(2)} & A_{13}^{(2)} & \cdots & 0 \\ 0 & A_{22}^{(2)} & A_{23}^{(2)} & \cdots & 0 \\ 0 & A_{32}^{(2)} & A_{33}^{(2)} & \cdots & 0 \\ \vdots & \vdots & \vdots & \cdots & \vdots \\ 0 & A_{N2}^{(2)} & A_{N3}^{(2)} & \cdots & 0 \end{bmatrix}
\tag{2.14}
$$

Using the recurrence relationship of weighting coefficient matrices

$$
\left[A^{(r)} \right] = \left[A^{(1)} \right]\left[A^{(r-1)} \right] = \left[A^{(r-1)} \right]\left[A^{(1)} \right]
\tag{2.15}
$$

we may obtain the modified weighting coefficient matrix of fourth-order derivative in the following way

$$
\left[\tilde{A}_{ij}^{(4)} \right] = \left[\tilde{A}_{ij}^{(2)} \right]\left[\tilde{A}_{ij}^{(2)} \right]
\tag{2.16}
$$

Consequently, let the quadrature analog of governing equation (2.8) be written in terms of modified weighting coefficients as follows

$$
\sum_{j=2}^{N-1} \tilde{A}_{ij}^{(4)} w_j = \Omega^2 w_i ; \quad i = 2,4,\ldots,(N\text{-}1)
\tag{2.17}
$$

In equation (2.17), the boundary conditions $d^2w/d\zeta^2 = 0$ at $\xi = 0$ and $\xi = 1$ are built in by modifying the weighting coefficient matrices. In order to satisfy the zero deflection boundary condition at each end of beam, $w = 0$ at $\zeta = 0$ and $\zeta = 1$, we ignore the sampling points $i=1$ and $i=N$ during writing the quadrature analog of governing equation as can be noted from equation (2.17).

The assembly of equation (2.17) for all values of the indices i and j results in the following eigenvalue equation which gives an $(N-2) \times (N-2)$ matrix

$$
[S]\{w\} - \Omega^2 [I]\{w\} = \{0\}
\tag{2.18}
$$

The eigenvalue matrix $[S]$ in equation (2.18) is comprised of modified weighting coefficients. As a result, ignoring the sampling points $i=1$ and $i=N$ enables satisfying

the zero deflection boundary condition at each end and, by modifying the second-order weighting coefficient matrix the zero moment boundary condition at each end is incorporated into the solution.

In this part of the present work, two commonly used approaches for implementing the boundary conditions into DQM solutions were introduced. One may see the reference [10] for the details of first explained approach for a beam problem. For the second approach of boundary condition implementation into DQM solutions, reference [8] is especially recommended for plate problems and also references [12] and [22] may be advised.

3. STATIC ANALYSIS OF PLATES BY DQM

In this section, static analyses of square plates are accomplished by DQM. Isotropic and laminated composite plates of constant and variable thickness are statically analyzed assuming the plates under distributed pressure force. Plates are assumed to be simply supported and clamped at four edges. In each sub-section, firstly the governing partial differential equation which gives the deflection of plate for the relevant plate configuration is given. Later, the DQM analog equations of them are presented using the rules given in section 2.1 to be solved. Numerical results that obtained from the derived DQM analog equations are given in section 6.

3.1 Isotropic Plate of Constant Thickness

Under the Kirchhoff's assumptions of the linear, elastic, small deflection theory of bending for thin plates of constant thickness, the governing differential equation for the deflections is as follows

$$\frac{\partial^4 w}{\partial x^4} + 2\frac{\partial^4 w}{\partial x^2 \partial y^2} + \frac{\partial^4 w}{\partial y^4} = \frac{p}{D} \tag{3.1}$$

where $w=w(x,y)$ is the deflection function, p is the pressure applied to upper surface of the plate and $D = Eh^3/12(1-\upsilon^2)$ is the flexural rigidity of the plate. Furthermore, E, h and υ are the modulus of elasticity, plate thickness and Poisson's ratio, respectively.

Before writing the DQM analogue equation of Eq. (3.1), it should be expressed in a non-dimensional form for convenience. The non-dimensional form of Eq. (3.1) would be expressed as following

$$\frac{\partial^4 W}{\partial X^4} + 2\lambda^2 \frac{\partial^4 W}{\partial X^2 \partial Y^2} + \lambda^4 \frac{\partial^4 W}{\partial Y^4} = \frac{pa^4}{D} \tag{3.2}$$

where $W = w / \alpha$ is the non-dimensional deflection (α being as a reference lenght); $X = x / a$, $Y = y / b$ are the non-dimensional coordinates; $\lambda = a / b$ is the aspect ratio of the plate and lastly a, b are the length and width of the plate along x and y coordinates, respectively.

In the all analyses of the present work two types of boundary conditions are analyzed: Clamped (C-C-C-C) and simply supported (S-S-S-S) on all four edges. For the clamped plate, the boundary conditions at each edge of plate can be expressed in dimensionless form as following

$$W(X,0) = W(X,1) = W(0,Y) = W(1,Y) = 0 \qquad \textbf{(3.3a)}$$

$$\frac{\partial W}{\partial X}(0,Y) = \frac{\partial W}{\partial X}(1,Y) = \frac{\partial W}{\partial Y}(X,0) = \frac{\partial W}{\partial Y}(X,1) = 0 \qquad \textbf{(3.3b)}$$

Equation (3.3.a) expresses the zero deflection at each plate edge whereas (3.3.b) states the zero slope at each plate edge.

Using same way, the boundary conditions of the simply supported plate on all four edges may be expressed in dimensionless form as following

$$W(X,0) = W(X,1) = W(0,Y) = W(1,Y) = 0 \qquad \textbf{(3.4a)}$$

$$\frac{\partial^2 W}{\partial X^2}(0,Y) = \frac{\partial^2 W}{\partial X^2}(1,Y) = \frac{\partial^2 W}{\partial Y^2}(X,0) = \frac{\partial^2 W}{\partial Y^2}(X,1) = 0 \qquad \textbf{(3.4b)}$$

Zero deflection and zero moment for the each simply supported edge of plate are expressed by the equations (3.4.a) and (3.4.b), respectively.

Introduction of DQM approximation rules Eqs. (2.1a) and (2.1b) into the dimensionless governing equation Eq. (3.2) yields the following DQM analog equation

$$\sum_{k=2}^{N_x-1} \tilde{A}_{ik}^{(4)} W_{kj} + 2\lambda^2 \sum_{k=2}^{N_x-1} \tilde{A}_{ik}^{(2)} \sum_{l=2}^{N_y-1} \tilde{B}_{jl}^{(2)} W_{kl} + \lambda^4 \sum_{l=2}^{N_y-1} \tilde{B}_{jl}^{(4)} W_{il} = \frac{pa^4}{D} \qquad \textbf{(3.5)}$$

where $i = 2,3, \ldots, (N_x\text{-}1)$ and $j = 2,3, \ldots, (N_y\text{-}1)$. In the Eq. (3.5), N_x and N_y are the number of grid points taken along the X and Y directions in the domain; $\tilde{A}_{ik}^{(r)}$ and $\tilde{B}_{jl}^{(r)}$ represent the modified weighting coefficients of x and y-type r-th order partial derivatives, respectively. As stated earlier the second approach that explained in section 2.3 is followed in this work for implementation of boundary conditions to the DQM solutions. That is to say, zero slope boundary condition for the clamped edges and zero moment for the simply supported edges is incorporated into the solution by modifying the weighting coefficient matrices. However, the grid points along X=0, X=1, Y=0 and Y=1 in Eq. (3.5) are ignored to take into account w=0 boundary condition at each edge and so, all the boundary conditions for the four edges (given by Eqs. (3.3) or (3.4)) are actually built into the governing equation. See the reference [8] for the details of the abovementioned boundary conditions incorporating procedure.

Expanding Eq. (3.5) for all values of the indices i and j a matrix of size $(N_x - 2)^2 \times (N_y - 2)^2$ is obtained to be solved in order to obtain the deflections at each grid point taken on the plate. At the present study FORTRAN programs were developed to solve all these types of DQM equations.

3.2 Layered Composite Plate of Constant Thickness

In this section, the governing differential equation and its DQM analog equation regarding the deflection analysis of anisotropic plates are represented. The governing differential equation for deflection analysis of orthotropic layered thin composite plate may be expressed as following

$$D_{11}\frac{\partial^4 w}{\partial x^4} + 4D_{16}\frac{\partial^4 w}{\partial x^3 \partial y} + \left(2D_{12} + 4D_{66}\right)\frac{\partial^4 w}{\partial x^2 \partial y^2} + $$
$$4D_{26}\frac{\partial^4 w}{\partial x \partial y^3} + D_{22}\frac{\partial^4 w}{\partial y^4} = p \tag{3.6}$$

In equation (3.6), the D_{ij}'s are the coefficients of flexural rigidity of the composite plate. For the calculation of these coefficients one may see any textbook that involves mechanics of composite structures, see for instance, reference [30]. We can make use of the same approach used in the Section 3.1 in order to obtain the dimensionless form of Eq. (3.6). So, we obtain

$$\frac{\partial^4 W}{\partial X^4} + 4\lambda^4 \frac{D_{16}}{D_{11}} \frac{\partial^4 W}{\partial X^3 \partial Y} + \lambda^2 \frac{(2D_{12} + 4D_{66})}{D_{11}} \frac{\partial^4 W}{\partial X^2 \partial Y^2} + 4\lambda^3 \frac{D_{26}}{D_{11}} \frac{\partial^4 W}{\partial X \partial Y^3} +$$

$$\lambda^4 \frac{D_{22}}{D_{11}} \frac{\partial^4 W}{\partial Y^4} = \frac{pa^4}{D_{11}}$$

(3.7)

Introduction of DQM approximation rules Eqs. (2.1a) and (2.1b) into the dimensionless governing differential equation Eq. (3.7) yields the following DQM analog equation for the deflection analysis of layered composite plate

$$\sum_{k=2}^{N_x-1} \tilde{A}_{ik}^{(4)} W_{kj} + 4\lambda \frac{D_{16}}{D_{11}} \sum_{k=2}^{N_x-1} \tilde{A}_{ik}^{(3)} \sum_{l=2}^{N_y-1} \tilde{B}_{jl}^{(1)} W_{kl} + \lambda^2 \frac{2D_{12} + 4D_{66}}{D_{11}} \sum_{k=2}^{N_x-1} \tilde{A}_{ik}^{(2)} \sum_{l=2}^{N_y-1} \tilde{B}_{jl}^{(2)} W_{kl}$$

$$+4\lambda^3 \frac{D_{26}}{D_{11}} \sum_{k=2}^{N_x-1} \tilde{A}_{ik}^{(1)} \sum_{l=2}^{N_y-1} \tilde{B}_{jl}^{(3)} W_{kl} + \lambda^4 \frac{D_{22}}{D_{11}} \sum_{l=2}^{N_y-1} \tilde{B}_{jl}^{(4)} W_{il} = \frac{pa^4}{D_{11}}$$

(3.8)

for $i = 2,3, \ldots, (N_x\text{-}1)$ and $j = 2,3, \ldots, (N_y\text{-}1)$. In the case of a plate with specially orthotropic material properties, the coupling vanishes between bending and twisting stiffness components (i.e., $D_{16} = D_{26} = 0$) [18]. In this situation, the governing equation, Eq. (3.8), simplifies to

$$\sum_{k=2}^{N_x-1} \tilde{A}_{ik}^{(4)} W_{kj} + \lambda^2 \frac{2D_{12} + 4D_{66}}{D_{11}} \sum_{k=2}^{N_x-1} \tilde{A}_{ik}^{(2)} \sum_{l=2}^{N_y-1} \tilde{B}_{jl}^{(2)} W_{kl}$$

$$+\lambda^4 \frac{D_{22}}{D_{11}} \sum_{l=2}^{N-1} \tilde{B}_{jl}^{(4)} W_{il} = \frac{pa^4}{D_{11}}$$

(3.9)

In the present work all the plates that investigated are assumed to be specially-orthotropic. The equations of applied boundary conditions are given by Eqs. (3.3) for fully clamped plate, and Eqs. (3.4) for fully simply supported plate. However, these boundary conditions are incorporated into the solution by modifying the weighting coefficients matrices and ignoring the grid points along X=0, X=1, Y=0 and Y=1 as told in the section 2.3. We obtain a matrix of size $(N_x - 2)^2 \times (N_y - 2)^2$ from expansion of Eq. (3.8) or (3.9) to be solved in order to obtain the deflections at each grid point taken on the plate.

3.3 Isotropic Plate of Variable Thickness

In this section, a rectangular isotropic plate with linearly varying thickness is considered. For simplicity, the variation is assumed just along the *x*-axis. The procedure given by Farsa [17] and Kukreti at al. [18] is quite convenient to follow in order to obtain the governing differential equation for the deflection analysis of tapered isotropic plate.

The general differential equation governing the deflection analysis of a genaral tapered plate may be deduced from Ref. [17, 18] as follows

$$
\bar{D}\left(\frac{\partial^4 w}{\partial x^4} + 2\frac{\partial^4 w}{\partial x^2 \partial y^2} + \frac{\partial^4 w}{\partial y^4}\right) + 2\frac{\partial \bar{D}}{\partial x}\left(\frac{\partial^3 w}{\partial x^3} + \frac{\partial^3 w}{\partial x \partial y^2}\right)
$$
$$
+2\frac{\partial \bar{D}}{\partial y}\left(\frac{\partial^3 w}{\partial x^2 \partial y} + \frac{\partial^3 w}{\partial y^3}\right) + \frac{\partial^2 \bar{D}}{\partial x^2}\left(\frac{\partial^2 w}{\partial x^2} + \upsilon\frac{\partial^2 w}{\partial y^2}\right) \qquad (3.10)
$$
$$
+2(1-\upsilon)\frac{\partial^2 \bar{D}}{\partial x \partial y}\frac{\partial^2 w}{\partial x \partial y} + \frac{\partial^2 \bar{D}}{\partial y^2}\left(\upsilon\frac{\partial^2 w}{\partial x^2} + \frac{\partial^2 w}{\partial y^2}\right) = p
$$

where $\bar{D}$ is the flexural rigidity of the plate which is a function of *x* and *y*, and υ is the Poisson's ratio. As were in previous sections we nondimensionalize the variables and then apply the DQM rules to Eq. (3.10) and obtain the following DQM analog equation

$$
\bar{\bar{D}}\left(\sum_{k=2}^{N_x-1}\tilde{A}_{ik}^{(4)}W_{kj} + 2\lambda^2\sum_{k=2}^{N_x-1}\tilde{A}_{ik}^{(2)}\sum_{l=2}^{N_y-1}\tilde{B}_{jl}^{(2)}W_{kl} + \lambda^4\sum_{l=2}^{N_y-1}\tilde{B}_{jl}^{(4)}W_{il}\right)
$$
$$
+2\bar{\bar{D}}_{,X}\left(\sum_{k=2}^{N_x-1}\tilde{A}_{ik}^{(3)}W_{kj} + \lambda^2\sum_{k=2}^{N_x-1}\tilde{A}_{ik}^{(1)}\sum_{l=2}^{N_y-1}\tilde{B}_{jl}^{(2)}W_{kl}\right)
$$
$$
+2\bar{\bar{D}}_{,Y}\left(\lambda^2\sum_{k=2}^{N_x-1}\tilde{A}_{ik}^{(2)}\sum_{l=2}^{N_y-1}\tilde{B}_{jl}^{(1)}W_{kl} + \lambda^4\sum_{l=2}^{N_y-1}\tilde{B}_{jl}^{(3)}W_{il}\right)
$$
$$
\qquad (3.11)
$$
$$
+\bar{\bar{D}}_{,XX}\left(\sum_{k=2}^{N_x-1}\tilde{A}_{ik}^{(2)}W_{kj} + \upsilon\lambda^2\sum_{l=2}^{N_y-1}\tilde{B}_{jl}^{(2)}W_{il}\right)
$$
$$
+2(1-\upsilon)\bar{\bar{D}}_{,XY}\lambda^2\sum_{k=2}^{N_x-1}\tilde{A}_{ik}^{(1)}\sum_{l=2}^{N_y-1}\tilde{B}_{jl}^{(1)}W_{kl}
$$
$$
+\bar{\bar{D}}_{,YY}\left(\upsilon\lambda^2\sum_{k=2}^{N_x-1}\tilde{A}_{ik}^{(2)}W_{kj} + \lambda^4\sum_{l=2}^{N_y-1}\tilde{B}_{jl}^{(2)}W_{il}\right) = pa^4
$$

where $\overline{\overline{D}}$ is the flexural rigidity function of the plate expressed with respect to nondimensional X- and Y-coordinates. Other terms in the Eq. (3.11) had also been explained in previous sections.
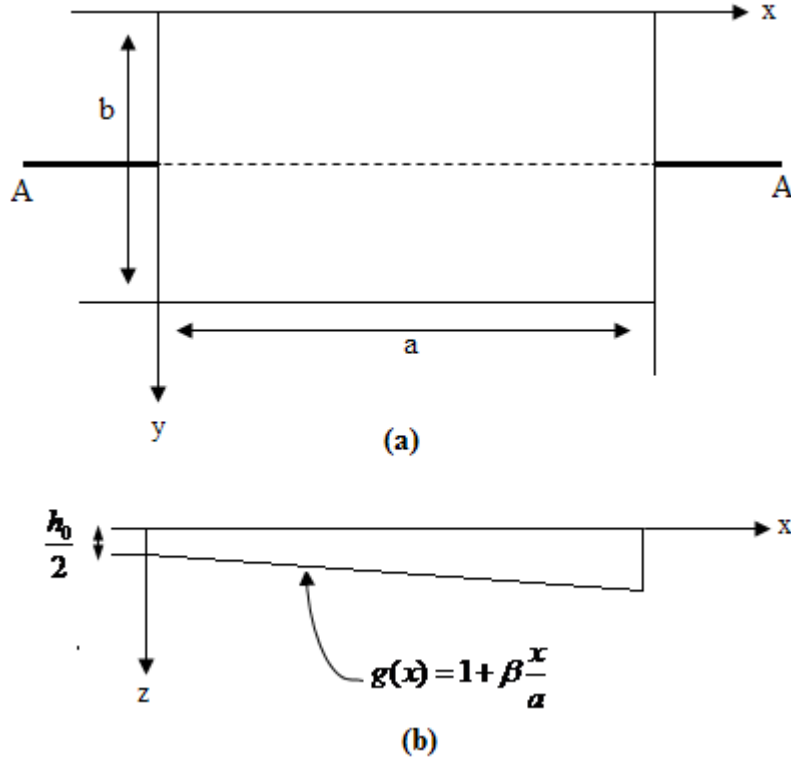
Fig. 3.1: Geometry of isotropic tapered plate:
(a) Plan view; (b) Half cross section A-A

As stated earlier, thickness variation is assumed to be along x-axis as shown in figure 3.1 (b). Considering the thickness variation as

$$h = h_0 g(x) \tag{3.12}$$

where h_0 is the thickness at the origin; and

$$g(x) = 1 + \beta \frac{x}{a} \text{ for } 0 \le x \le a \tag{3.13}$$

where β is the taper ratio parameter which defines the thickness variation. Nondimensionalizing the Eqs. (3.12) and (3.13) yields

$$h = h_0 G(X) \tag{3.14}$$

$$G(X) = 1 + \beta X \text{ for } 0 \le X \le 1 \tag{3.15}$$

Using this nomenclature we can express the nondimensional flexural rigidity of the plate as follows

$$\overline{\overline{D}} = D_0 G^3(X) \text{ for } 0 \le X \le 1 \tag{3.16}$$

where $D_0 = h_0^3 E / 12(1-\upsilon^2)$. Here h_0 denotes the thickness at the plate origin. Substituting Eqs. (3.15) and (3.16) into Eq. (3.11) gives the governing equation of a plate with linearly varying thickness along the x-axis for deflection analysis

$$
(1+\beta X_i)^2 \left(\sum_{k=2}^{N_x-1} \tilde{A}_{ik}^{(4)} W_{kj} + 2\lambda^2 \sum_{k=2}^{N_x-1} \tilde{A}_{ik}^{(2)} \sum_{l=2}^{N_y-1} \tilde{B}_{jl}^{(2)} W_{kl} + \lambda^4 \sum_{l=2}^{N_y-1} \tilde{B}_{jl}^{(4)} W_{il} \right)
$$
$$
+6\beta(1+\beta X_i) \left(\sum_{k=2}^{N_x-1} \tilde{A}_{ik}^{(3)} W_{kj} + \lambda^2 \sum_{k=2}^{N_x-1} \tilde{A}_{ik}^{(1)} \sum_{l=2}^{N_y-1} \tilde{B}_{jl}^{(2)} W_{kl} \right) \tag{3.17}
$$
$$
+6\beta^2 \left(\sum_{k=2}^{N_x-1} \tilde{A}_{ik}^{(2)} W_{kj} + \upsilon\lambda^2 \sum_{l=2}^{N_y-1} \tilde{B}_{jl}^{(2)} W_{il} \right) = \frac{pa^4}{D_0}
$$

for $i = 2,3, \ldots, (N_x\text{-}1)$ and $j = 2,3, \ldots, (N_y\text{-}1)$. Equation (3.17) was solved for fully simply supported and clamped plates. The related boundary conditions are given by Eqs. (3.3) or (3.4) are built into the governing equation via modifying the weighting coefficients matrices and ignoring the grid points along X=0, X=1, Y=0 and Y=1. By doing so, a matrix of size $(N_x-2)^2 \times (N_y-2)^2$ is obtained to be solved.

3.4 Layered Composite Plate of Variable Thickness

In this section, a different way is followed compared to the previous section due to the material selection for the tapered plate. To explain the way briefly, the DQM analog equations, which for composite plates of constant thickness, are written down including the calculated flexural stiffness of plate, one by one, on each grid points of the tapered plate. That is to say, the flexural stiffness, which changes linearly along the x-axis of plate, is incorporated into the governing DQM analogue equation at each grid point during the formulation. Following formulation can be proposed for the regarding analysis:

$$\left(D_{11}\right)_{ij} \mathrm{K}_{ij} = Pa^4 \tag{3.18}$$

where

$$K_{ij} = \sum_{k=2}^{N_x-1} \tilde{A}_{ik}^{(4)} W_{kj} + 4\lambda \frac{D_{16}}{D_{11}} \sum_{k=2}^{N_x-1} \tilde{A}_{ik}^{(3)} \sum_{l=2}^{N_y-1} \tilde{B}_{jl}^{(1)} W_{kl} +$$

$$\lambda^2 \frac{2D_{12}+4D_{66}}{D_{11}} \sum_{k=2}^{N_x-1} \tilde{A}_{ik}^{(2)} \sum_{l=2}^{N_y-1} \tilde{B}_{jl}^{(2)} W_{kl} +$$

$$4\lambda^3 \frac{D_{26}}{D_{11}} \sum_{k=2}^{N_x-1} \tilde{A}_{ik}^{(1)} \sum_{l=2}^{N_y-1} \tilde{B}_{jl}^{(3)} W_{kl} + \lambda^4 \frac{D_{22}}{D_{11}} \sum_{l=2}^{N_y-1} \tilde{B}_{jl}^{(4)} W_{il}$$

for $i = 2,3, \ldots, (N_x\text{-}1)$ and $j = 2,3, \ldots, (N_y\text{-}1)$. The i, j indices in the term $\left(D_{11}\right)_{ij}$ indicates that it is written with respect to the plate thickness of the regarding grid point on the plate. As was in earlier sections the boundary conditions given by equations (3.3) or (3.4) are built into the governing equation via modifying the weighting coefficients matrices and ignoring the grid points along X=0, X=1, Y=0 and Y=1. By doing so, a matrix of size $(N_x - 2)^2 \times (N_y - 2)^2$ is obtained to be solved.

4. FREE VIBRATION ANALYSIS OF PLATES BY DQM

Free vibration analyses of aforementioned plates have been achieved in this section. For each plate configuration, the equations governing the free flexural vibration of plates of constant thickness and variable thickness made of isotropic and layered composite materials are given firstly. Furthermore, the DQM analog equations are derived to be solved numerically applying the DQM rules to each governing equation in the each sub-section.

4.1 Isotropic Plates of Constant Thickness

The differential equation governing the free flexural vibration of a thin rectangular plate of isotropic materials, in terms of lateral displacement, w, can be written as

$$D\left(\frac{\partial^4 w(x,y,t)}{\partial x^4} + 2\frac{\partial^4 w(x,y,t)}{\partial x^2 \partial y^2} + \frac{\partial^4 w(x,y,t)}{\partial y^4}\right) + \rho h \frac{\partial^2 w(x,y,t)}{\partial t^2} = 0 \qquad (4.1)$$

where D is the flexural stiffness of the plate, ρ is the density of the plate material, h is the plate thickness and t represents the time. Assuming a function which gives harmonically periodic time response for the displacement, for example taking $w(x,y,t) = w(x,y)\cos\omega t$ where ω is the dimensional circular frequency, and substituting into Eq. (4.1) results

$$D\left(\frac{\partial^4 w(x,y)}{\partial x^4} + 2\frac{\partial^4 w(x,y)}{\partial x^2 \partial y^2} + \frac{\partial^4 w(x,y)}{\partial y^4}\right) - \rho h \omega^2 w(x,y) = 0 \qquad (4.2)$$

Making the variables nondimensional in Eq. (4.2) yields

$$\frac{\partial^4 W}{\partial X^4} + 2\lambda^2 \frac{\partial^4 W}{\partial X^2 \partial Y^2} + \lambda^4 \frac{\partial^4 W}{\partial Y^4} - \Omega^2 W = 0 \qquad (4.3)$$

where $W = W(X,Y)$ is the dimensionless mode function corresponds to the dimensionless frequency Ω; $X = x/a$, $Y = y/b$ are dimensionless coordinates; a and b are the lengths of the plate edges parallel to the x and y axes, respectively;

21

$\lambda = a/b$ is the aspect ratio, and $\Omega = \omega a^2 \sqrt{\rho h/D}$. Further, $D = h^3 E/12(1 - \upsilon^2)$ where E and υ are the Young's modulus and Poisson's ratio, respectively. Subsequently, applying the DQ rules Eqs. (2.1) to Eq. (4.3) and using the boundary condition approach used in the previous chapters in which the boundary conditions are applied during formulation of the weighting coefficients yield

$$\sum_{k=2}^{N_x-1} \tilde{A}_{ik}^{(4)} W_{kj} + 2\lambda^2 \sum_{k=2}^{N_x-1} \tilde{A}_{ik}^{(2)} \sum_{l=2}^{N_y-1} \tilde{B}_{jl}^{(2)} W_{kl} + \lambda^4 \sum_{l=2}^{N_y-1} \tilde{B}_{jl}^{(4)} W_{il} - \Omega^2 W_{ij} = 0 \qquad \textbf{(4.4)}$$

for $i = 2,3, \ldots, (N_x\text{-}1)$ and $j = 2,3, \ldots, (N_y\text{-}1)$. The assembly of Eq. (4.4) for all values of the indices i and j results in the following eigenvalue equation of size $(N_x - 2) \times (N_y - 2)$

$$[S]\{W\} - \Omega^2 [I]\{W\} = 0 \qquad \textbf{(4.5)}$$

where the eigenvalue matrix $[S]$ is comprised of the modified weighting coefficients [8]. Solving Eq. (4.5) numerically gives the dimensionless eigenvalues.

4.2 Laminated Composite Plates of Constant Thickness

The differential equation governing the free flexural vibration of a mid-plane symmetric laminated orthotropic rectangular plate of constant thickness can be written in dimensionless form as following [20]

$$\frac{\partial^4 W}{\partial X^4} + 4\lambda^4 \frac{D_{16}}{D_{11}} \frac{\partial^4 W}{\partial X^3 \partial Y} + \lambda^2 \frac{(2D_{12} + 4D_{66})}{D_{11}} \frac{\partial^4 W}{\partial X^2 \partial Y^2} + 4\lambda^3 \frac{D_{26}}{D_{11}} \frac{\partial^4 W}{\partial X \partial Y^3}$$
$$+ \lambda^4 \frac{D_{22}}{D_{11}} \frac{\partial^4 W}{\partial Y^4} - \Omega^2 W = 0 \qquad \textbf{(4.6)}$$

where $W = W(X,Y)$ is the dimensionless mode function corresponding to dimensionless frequency Ω; $X = x/a$, $Y = y/b$ are dimensionless coordinates; $\lambda = a/b$ is the aspect ratio; D_{ij}'s are the flexural rigidities of the composite plate; a and b are the lengths of rectangular plates parallel to x and y axis, respectively. Furthermore, $\Omega^2 = \omega^2 a^4 (\rho h/D_{11})$ where ω is the dimensional circular frequency and h is the plate thickness. DQM analog equation of Eq. (4.6) can be written as

$$\sum_{k=2}^{N_x-1} \tilde{A}_{ik}^{(4)} W_{kj} + 4\lambda \frac{D_{16}}{D_{11}} \sum_{k=2}^{N_x-1} \tilde{A}_{ik}^{(3)} \sum_{l=2}^{N_y-1} \tilde{B}_{jl}^{(1)} W_{kl} +$$

$$\lambda^2 \frac{2D_{12}+4D_{66}}{D_{11}} \sum_{k=2}^{N_x-1} \tilde{A}_{ik}^{(2)} \sum_{l=2}^{N_y-1} \tilde{B}_{jl}^{(2)} W_{kl}$$

$$+4\lambda^3 \frac{D_{26}}{D_{11}} \sum_{k=2}^{N_x-1} \tilde{A}_{ik}^{(1)} \sum_{l=2}^{N_y-1} \tilde{B}_{jl}^{(3)} W_{kl} +$$

$$\lambda^4 \frac{D_{22}}{D_{11}} \sum_{l=2}^{N_y-1} \tilde{B}_{jl}^{(4)} W_{il} - \Omega^2 W_{ij} = 0$$

(4.7)

for $i = 2, 3, \ldots, (N_x\text{-}1)$ and $j = 2, 3, \ldots, (N_y\text{-}1)$. The assembly of Eq. (4.7) for all values of the indices i and j results in an eigenvalue equation of size $(N_x - 2) \times (N_y - 2)$ like Eq. (4.5) to be solved. The free vibration frequencies of simply supported (S-S-S-S) and clamped (C-C-C-C) laminated composite plates are obtained by solving Eq. (4.7). Numerical results are given in section 6.

4.3 Isotropic Plate of Variable Thickness

We can utilize the same manner used in Section (3.3) in order to obtain the governing equation for freely vibrating isotropic thin tapered plate. We again make the same assumption for the motion of the plate that it is harmonically periodic in time. Furthermore, we again assume that the thickness variation is just along the x-axis and it is linear of which function is given by Eq. (3.12). Modifying Eq. (3.17) for free vibration analysis of the plate results in following DQM analog eigenvalue equation

$$(1+\beta X_i)^2 \left(\sum_{k=2}^{N_x-1} \tilde{A}_{ik}^{(4)} W_{kj} + 2\lambda^2 \sum_{k=2}^{N_x-1} \tilde{A}_{ik}^{(2)} \sum_{l=2}^{N_y-1} \tilde{B}_{jl}^{(2)} W_{kl} + \lambda^4 \sum_{l=2}^{N_y-1} \tilde{B}_{jl}^{(4)} W_{il} \right)$$

$$+6\beta(1+\beta X_i) \left(\sum_{k=2}^{N_x-1} \tilde{A}_{ik}^{(3)} W_{kj} + \lambda^2 \sum_{k=2}^{N_x-1} \tilde{A}_{ik}^{(1)} \sum_{l=2}^{N_y-1} \tilde{B}_{jl}^{(2)} W_{kl} \right)$$

(4.8)

$$+6\beta^2 \left(\sum_{k=2}^{N_x-1} \tilde{A}_{ik}^{(2)} W_{kj} + \upsilon\lambda^2 \sum_{l=2}^{N_y-1} \tilde{B}_{jl}^{(2)} W_{il} \right) - \Omega^2 W_{ij} = 0$$

23

for $i = 2, 3, \ldots, (N_x\text{-}1)$ and $j = 2, 3, \ldots, (N_y\text{-}1)$. In Eq. (4.8), $W=W(X,Y)$ is the dimensionless mode function corresponding to dimensionless frequency Ω; $X=x/a$, $Y=y/b$ are dimensionless coordinates; $\lambda = a/b$ is the aspect ratio; a and b are the lengths of rectangular plates parallel to x and y axis, respectively. Furthermore, $\Omega^2 = \omega^2 a^4 (\rho h_0 / D_0)$ where ω is the dimensional circular frequency; ρ is the density of plate material; h_0 is the plate thickness at the plate origin (see figure 3.1), and $D_0 = h_0^3 E / 12(1-\upsilon^2)$. Again, the boundary conditions given by Eqs. (3.3) or (3.4) are built into the governing equation via modifying the weighting coefficients matrices and ignoring the grid points along $X=0$, $X=1$, $Y=0$ and $Y=1$. By doing so, a set of equations of size $(N_x - 2) \times (N_y - 2)$ is obtained to be solved from the assembly of Eq. (4.8) for all values of the indices i and j.

4.4 Laminated Composite Plate of Variable Thickness

As was in section 3.4 a different approach is followed in this section compared to the sections involve isotropic tapered plate in the analyses. In the Sections (3.3) and (4.3), a linear function was assumed for the plate thickness and was substituted into a general governing equation which involves the derivatives of the plate rigidities. Consequently, a governing equation was obtained which just involves the plate taper ratios at the grid points and the plate rigidity at the plate origin. However, the case where a laminated composite plate takes place in the analyses of plates of variable thickness might make the derivation of an analytical equation that governs the behaviour of the regarding plate quite complex. In this case, we approached the problem from a probable production way of such a plate. Noting that the governing equation given in the Section 3.4 for the case of deflection analysis of tapered laminated composite plates, the free vibration equation can also be written in the following form:

$$\left(\frac{D_{11}}{h} \right)_{ij} K_{ij} W_{ij} - \Omega^2 W_{ij} = 0 \qquad (4.9)$$

where

$\Omega = \omega a^2 \sqrt{\rho}$ is a dimensional frequency parameter from which the circular frequency ω can be obtained and

$$K_{ij} = \sum_{k=2}^{N_x-1} \tilde{A}_{ik}^{(4)} W_{kj} + 4\lambda \frac{D_{16}}{D_{11}} \sum_{k=2}^{N_x-1} \tilde{A}_{ik}^{(3)} \sum_{l=2}^{N_y-1} \tilde{B}_{jl}^{(1)} W_{kl} +$$

$$\lambda^2 \frac{2D_{12}+4D_{66}}{D_{11}} \sum_{k=2}^{N_x-1} \tilde{A}_{ik}^{(2)} \sum_{l=2}^{N_y-1} \tilde{B}_{jl}^{(2)} W_{kl} + \tag{4.10}$$

$$4\lambda^3 \frac{D_{26}}{D_{11}} \sum_{k=2}^{N_x-1} \tilde{A}_{ik}^{(1)} \sum_{l=2}^{N_y-1} \tilde{B}_{jl}^{(3)} W_{kl} + \lambda^4 \frac{D_{22}}{D_{11}} \sum_{l=2}^{N_y-1} \tilde{B}_{jl}^{(4)} W_{il}$$

for $i = 2,3, \ldots , (N_x$-1) and $j = 2,3, \ldots , (N_y$-1). The i, j indices in the term $\left(\dfrac{D_{11}}{h} \right)_{ij}$ in

Eq. (4.9) indicates that it is written with respect to the plate thickness of the regarding grid point on the plate. Again, the boundary conditions given by Eqs. (3.3) or (3.4) are built into the governing equation via modifying the weighting coefficients matrices and ignoring the grid points along X=0, X=1, Y=0 and Y=1. By doing so, a set of equations of size $(N_x - 2) \times (N_y - 2)$ is obtained to be solved.

5. TRANSIENT ANALYSES OF PLATES BY DQM

This chapter concerns with transient analyses of the aforementioned square plates. The plates are assumed to be exposed to air blast load. As were in the previous chapter, four different plate configurations are analyzed: Isotropic and laminated composite plates of constant and variable thicknesses. Plates are assumed to be fully clamped and simply supported. For the analysis of air blast loading, a function that approximates to the time variation of the blast pressure is assumed. The resulting governing equations, which are all time-dependent, are solved numerically using the Newmark time integration method. Hence, the Newmark time integration method is also explained in the first section before going into details of reference problems.

5.1 Isotropic Plate of Constant Thickness

The differential equation that governs the forced flexural vibration of an isotropic thin rectangular plate of Constant Thickness might be written as follows

$$D\left(\frac{\partial^4 w(x,y,t)}{\partial x^4} + 2\frac{\partial^4 w(x,y,t)}{\partial x^2 \partial y^2} + \frac{\partial^4 w(x,y,t)}{\partial y^4}\right) + \bar{m}\frac{\partial^2 w(x,y,t)}{\partial t^2} = p \qquad \textbf{(5.1)}$$

where $D = h^3 E / 12(1-\upsilon^2)$ is the flexural rigidity of the plate, $w(x,y,t)$ is the function governs displacement, $\bar{m} = \rho h$ is the mass per unit area of the plate, and p is the external force exposes on the plate. Substituting $W = w/\xi$ (ξ is a reference length), $X = x/a$, $Y = y/b$ into Eq. (5.1) in order to make the variables dimensionless yields

$$\frac{\partial^4 W}{\partial X^4} + 2\lambda^2 \frac{\partial^4 W}{\partial X^2 \partial Y^2} + \lambda^4 \frac{\partial^4 W}{\partial y^4} + \frac{a^4}{D}\bar{m}\frac{\partial^2 W}{\partial t^2} = \frac{pa^4}{D} \qquad \textbf{(5.2)}$$

where $\lambda = a/b$ is the aspect ratio of the plate and a and b are the lengths of the plate edges parallel to x and y axes, respectively. DQM analogue of Eq. (5.2) may be written using the quadrature rules given by Eqs. (2.1), as following

$$\sum_{k=2}^{N_x-1} \tilde{A}_{ik}^{(4)} W_{kj} + 2\lambda^2 \sum_{k=2}^{N_x-1} \tilde{A}_{ik}^{(2)} \sum_{l=2}^{N_y-1} \tilde{B}_{jl}^{(2)} W_{kl} + \lambda^4 \sum_{l=2}^{N_y-1} \tilde{B}_{jl}^{(4)} W_{il}$$

$$+ \frac{a^4}{D} \bar{m} (W_{ij})_{,tt} = \frac{pa^4}{D}$$

(5.3)

for $i = 2, 3, \ldots, (N_x\text{-}1)$ and $j = 2, 3, \ldots, (N_y\text{-}1)$. As were in previous analyses, the boundary conditions given by Eqs. (3.3) or (3.4) are built into the governing equation via modifying the weighting coefficients matrices and ignoring the grid points along $X=0$, $X=1$, $Y=0$ and $Y=1$. By doing so, a set of equations of size $(N_x - 2) \times (N_y - 2)$ is obtained from the assembly of Eq. (5.3) for all values of the indices i and j to be solved.

As was stated earlier, Newmark time integration method is used to solve Eq. (5.3). The Newmark time integration method can be described briefly as following:

If we assume a governing equation like following, time-dependent with external force,

$$\mathbf{M}\{\ddot{w}\} + \mathbf{K}\{w\} = \{F\}$$

(5.4)

where $\{w\}$ is the displacement vector; $\mathbf{M}$ is the mass matrix; $\ddot{w} = \partial^2 w / \partial t^2$; $\mathbf{K}$ is the stiffness matrix and $\{F\}$ is the load vector. The Newmark method uses finite difference expansions in the time interval Δt, in which it is assumed that

$$\{\dot{w}_{n+1}\} = \{\dot{w}_n\} \left[(1-\delta)\{\ddot{w}_n\} + \delta \ddot{w}_{n+1} \right] \Delta t$$

(5.5)

$$\{w_{n+1}\} = \{w_n\} + \{\dot{w}_n\} \Delta t + \left[(\frac{1}{2} - \alpha)\{\ddot{w}_n\} + \alpha \ddot{w}_{n+1} \right] \Delta t^2$$

(5.6)

where α and δ are Newmark integration parameters. To be able to figure out the displacements $\{w_{n+1}\}$, the governing Eq. (5.4) is evaluated at time t_{n+1} as

$$\mathbf{M}\{\ddot{w}_{n+1}\} + \mathbf{K}\{w_{n+1}\} = \{F\}$$

(5.7)

Rearranging Eqs. (5.5) and (5.6) as

$$\{\ddot{w}_{n+1}\} = a_0 (\{w_{n+1}\} - \{w_n\}) - a_2 \{\dot{w}_n\} - a_3 \{\ddot{w}_n\}$$

(5.8)

$$\{\dot{w}_{n+1}\} = \{\dot{w}_n\} + a_6 \{\ddot{w}_n\} + a_7 \{\ddot{w}_{n+1}\}$$

(5.9)

where $a_0 = 1/\alpha\Delta t^2$, $a_1 = \delta/\alpha\Delta t$, $a_2 = 1/\alpha\Delta t$, $a_3 = (1/2\alpha) - 1$, $a_4 = (\delta/\alpha) - 1$, $a_5 = (\Delta t/2)\{(\delta/\alpha) - 2\}$, $a_6 = \Delta t(1 - \delta)$, $a_7 = \delta\Delta t$ and combining the equations for $\{\ddot{w}_{n+1}\}$ and $\{\dot{w}_{n+1}\}$ with Eq. (5.7) yields the following equation from which the displacement at time t_{n+1} to be solved

$$(a_0\mathbf{M} + \mathbf{K})\{w_{n+1}\} = \{F\} + \mathbf{M}\left(a_0\{w_n\} + a_2\{\dot{w}_n\} + a_3\{\ddot{w}_n\}\right) \tag{5.10}$$

Once a solution is obtained for the displacement at time t_{n+1}, $\{w_{n+1}\}$, velocities and accelerations are updated as described in Eq. (5.8) and Eq. (5.9) in order to obtain the displacements at the further time steps. In the present transient analyses, the values $\alpha = 0.5$ and $\delta = 0.5$ are assumed for the Newmark time integration parameters. Furthermore, $\Delta t = 0.0001$ s is taken in the analyses.

It was stated earlier that the plate is assumed to be exposed to air blast load. For the regarding air blast load analysis, an approximation to the time variation of the blast pressure is given by Friedlander decay function as [1]

$$p(x, y, t) = p_m\left(1 - t/t_p\right)e^{-\alpha t/t_p} \tag{5.11}$$

In the present analyses, the parameters for the regarding Friedlander decay function are taken as in the Ref. [1], that is, $p_m = 28906 \, N/m^2$, $\alpha = 0.35$, $t_p = 0.0018s$. Consequently, what we have as the final governing equation to be solved when we apply the Newmark time integration method to the Eq. (5.3) and also substitute the air blast load function Eq. (5.11) as follows

$$\left(a_0\mathbf{M} + \frac{D}{a^4}\mathbf{K}\right)\{w_{n+1}\} = \{F\} + \mathbf{M}\left(a_0\{w_n\} + a_2\{\dot{w}_n\} + a_3\{\ddot{w}_n\}\right) \tag{5.12}$$

where

$$\mathbf{M} = \begin{bmatrix} \bar{m} & 0 & 0 & \\ 0 & \bar{m} & 0 & \ddots \\ 0 & 0 & \bar{m} & \ddots \\ & \ddots & \ddots & \ddots \end{bmatrix}$$

$$\mathbf{K} = \begin{bmatrix} K_{22} & K_{23} & \cdots & K_{2(Ny-1)} \\ K_{32} & K_{33} & \cdots & K_{3(Ny-1)} \\ \vdots & \vdots & \cdots & \vdots \\ K_{(Nx-1)2} & K_{(Nx-1)3} & \cdots & K_{(Nx-1)(Ny-1)} \end{bmatrix}$$

$$K_{ij} = \left(\sum_{k=2}^{N_x-1} \tilde{A}_{ik}^{(4)} W_{kj} + 2\lambda^2 \sum_{k=2}^{N_x-1} \tilde{A}_{ik}^{(2)} \sum_{l=2}^{N_y-1} \tilde{B}_{jl}^{(2)} W_{kl} + \lambda^4 \sum_{l=2}^{N_y-1} \tilde{B}_{jl}^{(4)} W_{il} \right)$$

for $i = 2, 3, \ldots, (N_x\text{-}1)$ and $j = 2, 3, \ldots, (N_y\text{-}1)$ and

$$F_{ij} = p_m \left(1 - t/t_p \right) e^{-\alpha t/t_p}$$

for $t = 0.0, 0.0001, 0.0002, \ldots, 0.01$.

It should be noted that we obtain dimensional displacements from Eq. (5.12) since the entire equation is multiplied by D/a^4. The applied boundary conditions given by Eq. (3.3) and Eq. (3.4) are built into the governing equation via modifying the weighting coefficients matrices and ignoring the grid points along X=0, X=1, Y=0 and Y=1. Furthermore, it can be noted that a matrix of size $(N_x - 2)^2 \times (N_y - 2)^2$ is obtained at each time increment from the left-hand side of assembly of Eq. (5.12) of which solution gives the displacements at the each grid point on the plate at each time increment. In the present study, the strains are also calculated using the displacements obtained at each time increment. The results are given in the next chapter as displacement-time and strain-time history graphs.

5.2 Layered Composite Plate of Constant Thickness

We may write the governing equation in the form of DQM formulation for the regarding analysis as following

$$\sum_{k=2}^{N_x-1} \tilde{A}_{ik}^{(4)} W_{kj} + 4\lambda \frac{D_{16}}{D_{11}} \sum_{k=2}^{N_x-1} \tilde{A}_{ik}^{(3)} \sum_{l=2}^{N_y-1} \tilde{B}_{jl}^{(1)} W_{kl} +$$

$$\lambda^2 \frac{2D_{12}+4D_{66}}{D_{11}} \sum_{k=2}^{N_x-1} \tilde{A}_{ik}^{(2)} \sum_{l=2}^{N_y-1} \tilde{B}_{jl}^{(2)} W_{kl}$$

$$+4\lambda^3 \frac{D_{26}}{D_{11}} \sum_{k=2}^{N_x-1} \tilde{A}_{ik}^{(1)} \sum_{l=2}^{N_y-1} \tilde{B}_{jl}^{(3)} W_{kl} +$$

$$\lambda^4 \frac{D_{22}}{D_{11}} \sum_{l=2}^{N_y-1} \tilde{B}_{jl}^{(4)} W_{il} + \frac{a^4}{D} \bar{m} \frac{\partial^2 W_{ij}}{\partial t^2} = \frac{pa^4}{D}$$

(5.13)

for $i = 2, 3, \ldots, (N_x\text{-}1)$ and $j = 2, 3, \ldots, (N_y\text{-}1)$. Since all the terms in Eq. (5.13) have also been described in the previous sections we directly move on to solution of Eq. (5.13) applying the Newmark method explained in Section (5.1). Application of the Newmark time integration method to the Eq. (5.13) yields

$$\left(a_0 \mathbf{M} + \frac{D_{11}}{a^4} \mathbf{K} \right) \{w_{n+1}\} = \{F\} + \mathbf{M} \left(a_0 \{w_n\} + a_2 \{\dot{w}_n\} + a_3 \{\ddot{w}_n\} \right)$$

(5.14)

where

$$\mathbf{M} = \begin{bmatrix} \bar{m} & 0 & 0 & \\ 0 & \bar{m} & 0 & \ddots \\ 0 & 0 & \bar{m} & \ddots \\ & \ddots & \ddots & \ddots \end{bmatrix}$$

$$\mathbf{K} = \begin{bmatrix} K_{22} & K_{23} & \cdots & K_{2(Ny-1)} \\ K_{32} & K_{33} & \cdots & K_{3(Ny-1)} \\ \vdots & \vdots & \cdots & \vdots \\ K_{(Nx-1)2} & K_{(Nx-1)3} & \cdots & K_{(Nx-1)(Ny-1)} \end{bmatrix}$$

$$K_{ij} = \sum_{k=2}^{N_x-1} \tilde{A}_{ik}^{(4)} W_{kj} + 4\lambda \frac{D_{16}}{D_{11}} \sum_{k=2}^{N_x-1} \tilde{A}_{ik}^{(3)} \sum_{l=2}^{N_y-1} \tilde{B}_{jl}^{(1)} W_{kl} +$$

$$\lambda^2 \frac{2D_{12}+4D_{66}}{D_{11}} \sum_{k=2}^{N_x-1} \tilde{A}_{ik}^{(2)} \sum_{l=2}^{N_y-1} \tilde{B}_{jl}^{(2)} W_{kl}$$

$$+4\lambda^3 \frac{D_{26}}{D_{11}} \sum_{k=2}^{N_x-1} \tilde{A}_{ik}^{(1)} \sum_{l=2}^{N_y-1} \tilde{B}_{jl}^{(3)} W_{kl} +$$

$$\lambda^4 \frac{D_{22}}{D_{11}} \sum_{l=2}^{N_y-1} \tilde{B}_{jl}^{(4)} W_{il}$$

for $i = 2, 3, \ldots, (N_x\text{-}1)$ and $j = 2, 3, \ldots, (N_y\text{-}1)$ and

$$F_{ij} = p_m \left(1 - t/t_p\right) e^{-\alpha t/t_p}$$

for $t = 0.0, 0.0001, 0.0002, \ldots, 0.01$.

It should be pointed out, again, that displacements that are acquired from Eq. (5.14) are dimensional since the entire equation is multiplied by D_{11}/a^4. The boundary conditions given by Eqs. (3.3) and Eq. (3.4) are built into the governing equation via modifying the weighting coefficients matrices and ignoring the grid points along $X=0$, $X=1$, $Y=0$ and $Y=1$. Furthermore, it can be noted that a matrix of size $(N_x - 2)^2 \times (N_y - 2)^2$ is obtained at each time increment from the left-hand side of assembly of Eq. (5.14) of which solution gives the displacements at the each grid point on the plate at each time increment. In the present study, the strains are also calculated using the displacements obtained at each time increment. The results are given in the next chapter as displacement-time and strain-time history graphs.

5.3 Isotropic Plate of Variable Thickness

Making the same assumptions about the regarding plate as in the Sections (3.3) and (3.4), that is, the thickness variation is just along the *x*-axis and linear, the governing equation that governs the dynamic behaviour of an isotropic, tapered, thin rectangular plate subjected to air blast load can be written in the following DQM form

$$\left(a_0 \mathbf{M} + \frac{D_0}{a^4}\mathbf{K}\right)\{w_{n+1}\} = \{F\} + \mathbf{M}\left(a_0\{w_n\} + a_2\{\dot{w}_n\} + a_3\{\ddot{w}_n\}\right) \qquad (5.15)$$

where

$$\mathbf{M} = \begin{bmatrix} \bar{m}_{22} & 0 & 0 & \\ 0 & \bar{m}_{23} & 0 & \ddots \\ 0 & 0 & \bar{m}_{24} & \ddots \\ & \ddots & \ddots & \ddots \end{bmatrix} \qquad (5.16)$$

is the mass per unit area matrix, $m_{ij} = (\rho h)_{ij}$ and

$$
\mathbf{K} = \begin{bmatrix} K_{22} & K_{23} & \cdots & K_{2(Ny-1)} \\ K_{32} & K_{33} & \cdots & K_{3(Ny-1)} \\ \vdots & \vdots & \cdots & \vdots \\ K_{(Nx-1)2} & K_{(Nx-1)3} & \cdots & K_{(Nx-1)(Ny-1)} \end{bmatrix}
$$

$$
\begin{aligned}
K_{ij} = (1+\beta X_i)^2 & \left(\sum_{k=2}^{N_x-1} \tilde{A}_{ik}^{(4)} W_{kj} + 2\lambda^2 \sum_{k=2}^{N_x-1} \tilde{A}_{ik}^{(2)} \sum_{l=2}^{N_y-1} \tilde{B}_{jl}^{(2)} W_{kl} + \lambda^4 \sum_{l=2}^{N_y-1} \tilde{B}_{jl}^{(4)} W_{il} \right) \\
& + 6\beta(1+\beta X_i) \left(\sum_{k=2}^{N_x-1} \tilde{A}_{ik}^{(3)} W_{kj} + \lambda^2 \sum_{k=2}^{N_x-1} \tilde{A}_{ik}^{(1)} \sum_{l=2}^{N_y-1} \tilde{B}_{jl}^{(2)} W_{kl} \right) \qquad \textbf{(5.17)} \\
& + 6\beta^2 \left(\sum_{k=2}^{N_x-1} \tilde{A}_{ik}^{(2)} W_{kj} + \upsilon\lambda^2 \sum_{l=2}^{N_y-1} \tilde{B}_{jl}^{(2)} W_{il} \right)
\end{aligned}
$$

for $i = 2, 3, \ldots, (N_x\text{-}1)$ and $j = 2, 3, \ldots, (N_y\text{-}1)$ and

$$
F_{ij} = p_m \left(1 - t/t_p \right) e^{-\alpha t/t_p}
$$

for $t = 0.0, 0.0001, 0.0002, \ldots, 0.01$.

It is worth to point out especially that the mass per unit area is not constant for the regarding plate since it is tapered. Hence, the terms $\bar{m}_{ij}$ are numbered in Eq. (5.16) as can be noted in which each $\bar{m}_{ij}$ correspond a grid point on the plate domain. Furthermore, the term D_0 in Eq. (5.15) denotes the flexural stiffness of the plate at the plate origin and β represents the taper ratio of the plate as they were explained in the related previous sections.

As were in the last two sections, in which transient analyses of plates are carried out, the displacements that are acquired from Eq. (5.15) are dimensional. The boundary conditions given by Eq (3.3) and (3.4) are built into the governing equation via modifying the weighting coefficients matrices and ignoring the grid points along $X=0$, $X=1$, $Y=0$ and $Y=1$. Furthermore, it can be noted that a matrix of size $(N_x - 2)^2 \times (N_y - 2)^2$ is obtained at each time increment from the left-hand side of assembly of Eq. (5.15) of which solution gives the displacements at the each grid point on the plate at each time increment. In the present study, the strains are also calculated using the displacements obtained at each time increment. The results are given in the next chapter as displacement-time and strain-time history graphs.

5.4 Laminated Composite Plate of Variable Thickness

As noted in Sections (3.4) and (4.4) a different approach is followed in the solution of problem of a tapered laminated composite plate. The way that utilized in these sections involves much more numerical treatment rather than deriving the governing equations analytically and then the DQM analogues of them to be solved. The governing equations that also derived before for a laminated, orthotropic composite plate of constant thickness are utilized in a different way. To state more clearly, the DQM analogue equations, which for plates of constant thickness, are written down including the calculated flexural stiffnesses of plate, one by one, on each grid points of the tapered plate. That is to say, the flexural stiffnesses, which change linearly along the x-axis of plate, are incorporated into the governing DQM analog equation at each grid point during the formulation. Remembering the equations derived in earlier related sections, the governing equation to be used in the blast load analysis of laminated composite tapered plate may be expressed as follows

$$\left(a_0 \mathbf{M} + \left(\frac{D_{11}}{a^4} \right)_{ij} \mathbf{K} \right) \{w_{n+1}\} = \{F\} + \mathbf{M} \left(a_0 \{w_n\} + a_2 \{\dot{w}_n\} + a_3 \{\ddot{w}_n\} \right) \qquad \textbf{(5.18)}$$

where

$$\mathbf{M} = \begin{bmatrix} \bar{m}_{22} & 0 & 0 & \\ 0 & \bar{m}_{23} & 0 & \ddots \\ 0 & 0 & \bar{m}_{24} & \ddots \\ & \ddots & \ddots & \ddots \end{bmatrix} \qquad \textbf{(5.19)}$$

is the mass per unit area matrix, $m_{ij} = (\rho h)_{ij}$. However,

$$\mathbf{K} = \begin{bmatrix} K_{22} & K_{23} & \cdots & K_{2(Ny-1)} \\ K_{32} & K_{33} & \cdots & K_{3(Ny-1)} \\ \vdots & \vdots & \cdots & \vdots \\ K_{(Nx-1)2} & K_{(Nx-1)3} & \cdots & K_{(Nx-1)(Ny-1)} \end{bmatrix}$$

34

$$K_{ij} = \sum_{k=2}^{N_x-1} \tilde{A}_{ik}^{(4)} W_{kj} + 4\lambda \frac{D_{16}}{D_{11}} \sum_{k=2}^{N_x-1} \tilde{A}_{ik}^{(3)} \sum_{l=2}^{N_y-1} \tilde{B}_{jl}^{(1)} W_{kl} +$$

$$\lambda^2 \frac{2D_{12} + 4D_{66}}{D_{11}} \sum_{k=2}^{N_x-1} \tilde{A}_{ik}^{(2)} \sum_{l=2}^{N_y-1} \tilde{B}_{jl}^{(2)} W_{kl}$$

$$+ 4\lambda^3 \frac{D_{26}}{D_{11}} \sum_{k=2}^{N_x-1} \tilde{A}_{ik}^{(1)} \sum_{l=2}^{N_y-1} \tilde{B}_{jl}^{(3)} W_{kl} +$$

$$\lambda^4 \frac{D_{22}}{D_{11}} \sum_{l=2}^{N_y-1} \tilde{B}_{jl}^{(4)} W_{il}$$

(5.20)

for $i = 2, 3, \ldots, (N_x\text{-}1)$ and $j = 2, 3, \ldots, (N_y\text{-}1)$ and

$$F_{ij} = p_m \left(1 - t/t_p\right) e^{-\alpha t/t_p}$$

for $t = 0.0, 0.0001, 0.0002, \ldots, 0.01$. The i, j indices in the term $\left(\dfrac{D_{11}}{a^4}\right)_{ij}$ in Eq. (5.18) indicates that it is written with respect to the plate thickness of the regarding grid point on the plate. Again, the boundary conditions given by Eqs. (3.3) and (3.4) are built into the governing equation via modifying the weighting coefficients matrices and ignoring the grid points along $X=0$, $X=1$, $Y=0$ and $Y=1$. By doing so, a matrix of size $(N_x - 2)^2 \times (N_y - 2)^2$ is obtained to be solved.

6. RESULTS AND DISCUSSIONS

In the previous chapters, the DQM analog equations are derived from the governing equations of static, free vibration and transient analyses of various rectangular plates. Plates are analyzed from the aspects of material and plate thickness. Furthermore, two boundary conditions are considered in analyses: Simply supported (S-S-S-S) and clamped (C-C-C-C) on four edges. In this chapter, the numerical results that are obtained using the DQM governing analog equations that are derived for each analysis in the previous chapters are presented. Besides the obtained DQM results are compared with results of ANSYS which is finite element method based software. Additionally, some results have also been compared with some experimental, theoretical results that are available in literature.

6.1 Numerical Results for The Plates of Constant Thickness

Before presenting the numerical results, the material properties of plates are presented. In the analyses of this study two isotropic and three laminated composite materials are used. The properties of isotropic and laminated composite materials are given in Table 6.1 and Table 6.2, respectively. Laminated plates (M3 and M4) are seven-layered and the ply orientation angle is 0° for each layer. Third laminated plate (M5) is again seven layered and the stacking sequence is [0/90/0/90/0/90/0].

Table 6.1: Properties of isotropic materials.

Material	E (GPa)	υ	ρ (kg/m^3)
Aluminium (M1)	70	0.3	2700
Steel (M2)	207	0.3	7770

Table 6.2: Properties of composite materials.

Material	Bidirectional (M3)	Unidirectional (M4,M5)
E_1 (GPa)	24.14	40
E_2 (GPa)	24.14	10
G_{12} (GPa)	3.79	4.5
ν_{12}	0.11	0.27
ρ(kg/m^3)	1800	2000

The dimensionless centre deflections of the isotropic and laminated composite plates of constant thickness are given in Table 6.3 for the simply supported plate and in Table 6.4 for the clamped plate. As it can be noted from these tables, a good agreement is obtained between the results of DQM, ANSYS and literature for the plates of isotropic materials. However, there is a small discrepancy between the DQM and ANSYS results for the laminated composite plates. The dimensional deflections for symmetric, cross-ply specially orthotropic laminated plates can be obtained from $w = W(pa^4 / D_{11})$ (for isotropic materials D_{11} replaces with D).

Table 6.3: The dimensionless centre deflections (W) of the square plates (S-S-S-S) of constant thickness.

	Analytical [14]	DQM [9]	DQM	ANSYS
M1,M2	0.00406	0.00400	0.00406	0.00405
M3	---	---	0.00575	0.00582
M4	---	---	0.00886	0.00901
M5	---	---	0.00699	0.00722

Table 6.4: The dimensionless centre deflections (W) of the square plates (C-C-C-C) of constant thickness.

	Analytical [14]	DQM [9]	DQM	ANSYS
M1,M2	0.00126	0.00126	0.00126	0.00127
M3	---	---	0 .00146	0.00149
M4	---	---	0.00227	0.00231
M5	---	---	0.00181	0.00187

The fundamental dimensionless frequencies of isotropic and composite plates are given in Table 6.5 and Table 6.6 for simply supported and clamped plates of constant thickness, respectively. The plate aspect ratio is one for all cases. In Table 6.7, the

dimensionless free vibration frequencies for the first ten modes are given for isotropic plates of constant thickness. The results show that the free vibration frequencies are captured very well for the isotropic plates. The small discrepancy between the DQM and ANSYS results for the laminated composite plates can be attributed to the material model used in ANSYS. The material model used in ANSYS requires the material properties in the perpendicular direction to the plate. These material properties are chosen considering the matrix is dominated in the perpendicular direction and are given as E_3=3 GPa, G_{13}=G_{23}=1 GPa, ν_{13}=ν_{23}=0.4 [20]. There are also two numerical experiments achieved in Ref. [20] that explain the effect of the mentioned material model used in ANSYS on the results which might be assumed the reason of discrepancy between the DQM and ANSYS results. The dimensional frequency for symmetric, cross-ply specially orthotropic laminated plates considered here can be obtained from $\omega = (\Omega / a^2)\sqrt{D_{11} / \rho h}$, (for isotropic materials D_{11} replaces with D).

Table 6.5: The first dimensionless frequencies (Ω) of the square plates (S-S-S-S) of constant thickness.

	Analytical [14]	DQM [8]	DQM	ANSYS
M1,M2	19.739	19.738	19.739	19.709
M3	---	---	16.633	16.519
M4	---	---	13.339	13.228
M5	---	---	15.070	14.827

Table 6.6: The first dimensionless frequencies (Ω) of the square plates (C-C-C-C) of constant thickness.

	Analytical [14]	DQM [8]	DQM	ANSYS
M1,M2	35.992	35.989	35.985	35.856
M3	---	---	33.564	33.326
M4	---	---	26.667	26.416
M5	---	---	30.136	29.667

Table 6.7: The dimensionless frequencies (Ω) of the isotropic square plates of constant thickness for the first ten modes.

Mode	C-C-C-C		S-S-S-S	
	DQM	ANSYS	DQM	ANSYS
1	35.985	35.856	19.739	19.709
2	73.394	73.009	49.348	49.216
3	73.394	73.009	49.348	49.216
4	108.216	107.147	78.957	78.499
5	131.581	130.731	98.696	98.339
6	132.205	131.402	98.696	98.339
7	164.999	162.911	128.305	127.268
8	164.999	162.911	128.305	127.268
9	210.521	209.004	167.784	167.036
10	210.521	209.004	167.784	167.036

It can be seen in the Table 6.7 that the frequencies obtained using DQM are in an agreement with the frequencies obtained using ANSYS. However, there are small discrepancies at some modes. The free vibration frequencies obtained using DQM for the simply supported isotropic plates are in better agreement with ANSYS results for the first ten modes compared to the clamped plate. Generally, the results indicate that the stiffness of the laminated composite plate is predicted higher in DQM analysis compared to the prediction of ANSYS. In the DQM analysis, 15 grid points are used along the x and y axes on the plate domain ($N_x = N_y = 15$). In ANSYS, the isotropic plates are modelled using 14x14=196 shell elements (Shell63), and the laminated composite plates are modelled using 14x14=196 laminated shell elements (Shell99).

The centre deflections of the simply supported laminated plates of constant thickness are also obtained using the Navier's solution choosing the first 9 terms in the series solution. The results are given in Table 6.8. Results show that a better agreement is obtained between the DQM and ANSYS results. Furthermore it can be concluded that plates analyzed using Navier seem to behave stiffer than DQM and ANSYS.

Table 6.8: The dimensionless centre deflections (*W*) of the square
laminated plates (S-S-S-S) of constant thickness including
the Navier's solution.

	DQM	NAVIER	ANSYS
M3	0.00575	0.00440	0.00582
M4	0.00886	0.00684	0.00901
M5	0.00699	0.00509	0.00722

The displacement-time and strain-time histories of the plate centres are obtained
using the DQM and ANSYS for isotropic and laminated composite plates of constant
thickness of clamped and simply supported at all edges. The strain values in this
section represent the values of ε_X for each plate. Figure 6.1 and Figure 6.2 show the
displacement-time and strain-time histories of centre of the clamped aluminium plate
(M1) of constant thickness, respectively. DQM results are found to be in an
agreement with ANSYS and the other results found in the literature.
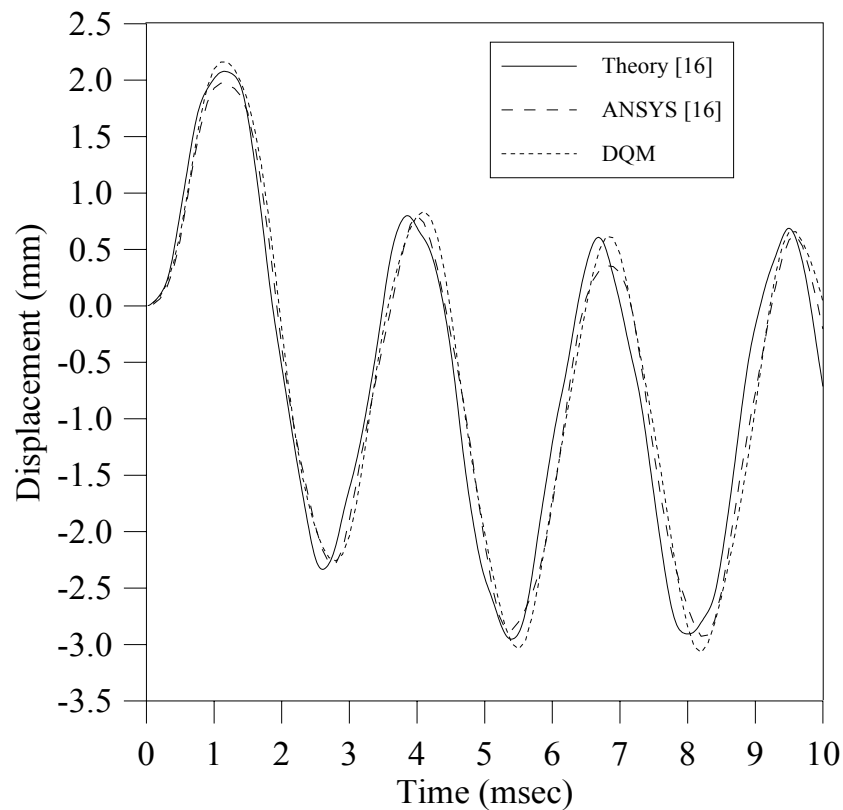
Figure 6.1: Displacement-time history of plate centre for the blast-loaded
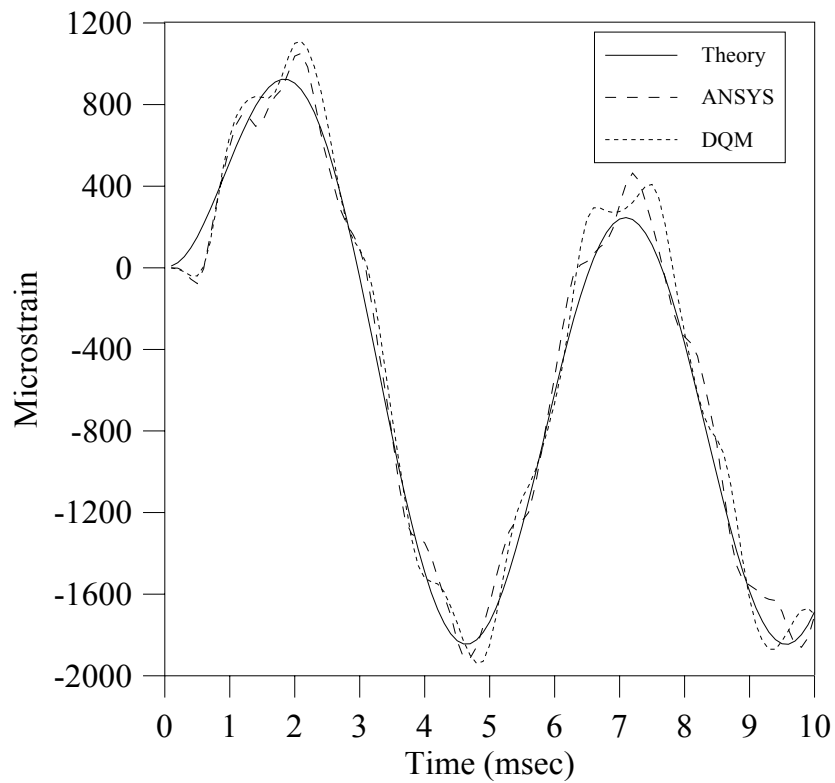clamped aluminium plate (M1) of constant thickness.
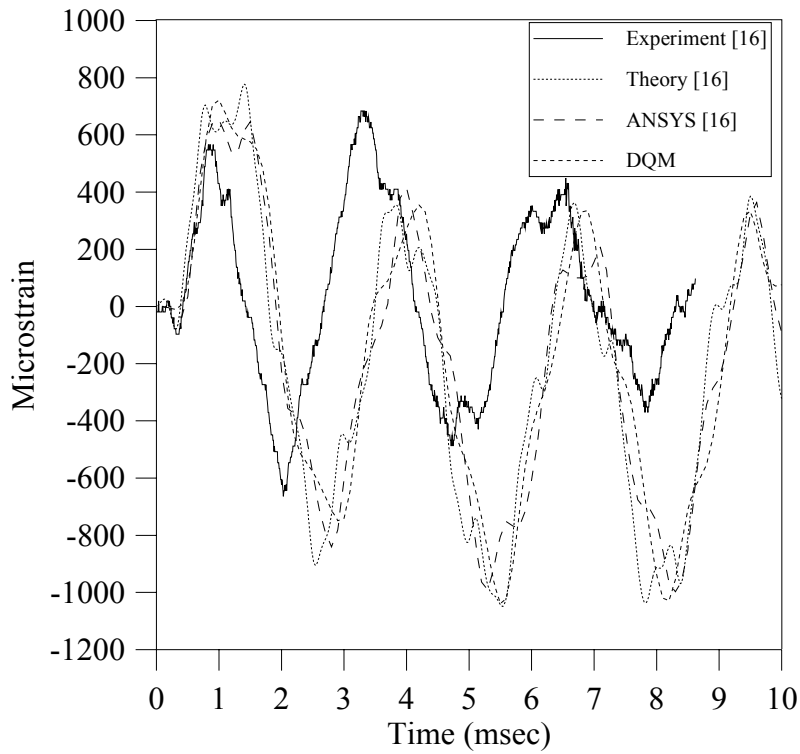
Figure 6.2: Strain-time history of plate centre for the blast-loaded
clamped aluminium plate (M1) of constant thickness.

The strain-time history result obtained for the clamped aluminium plate of constant thickness is also compared with the experimental result in Fig. 6.2 and a discrepancy is found between the experimental and predicted results. This discrepancy is because of the effect of nonlinear terms which are not included in the present study [20]. The theoretical and experimental results given in Figs. 6.1 and 6.2 are taken from Ref. [16].

Figure 6.3 and Figure 6.4 show displacement-time and the strain-time histories of the centre of simply supported aluminium plate (M1) of constant thickness, respectively. DQM results are found to be in an agreement with the ANSYS results and theoretical results taken from literature. The theoretical results for blast-loaded simply supported isotropic plates appear in Fig. 6.3 and 6.4 are taken from Ref. [21].
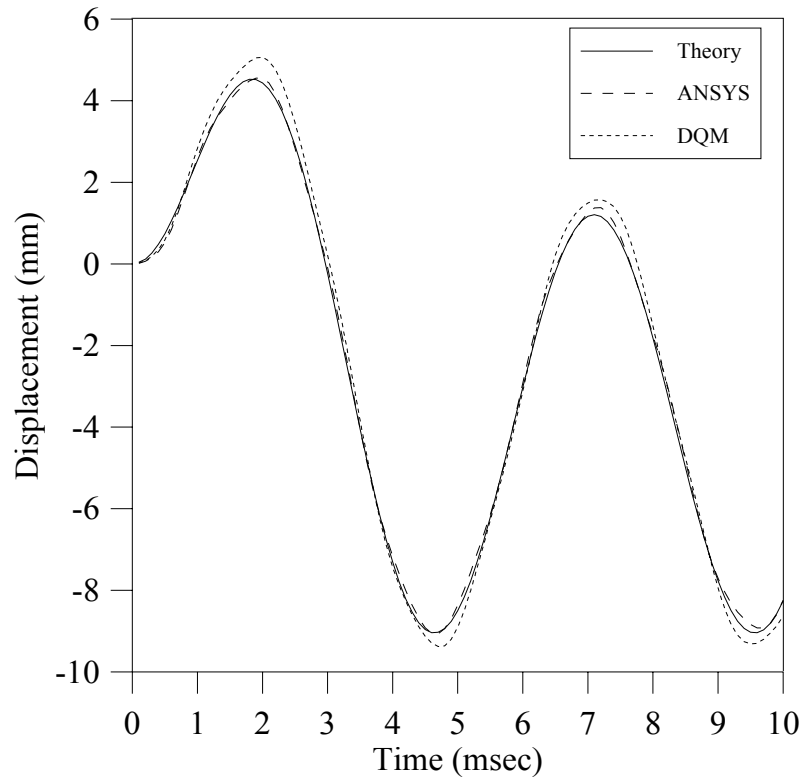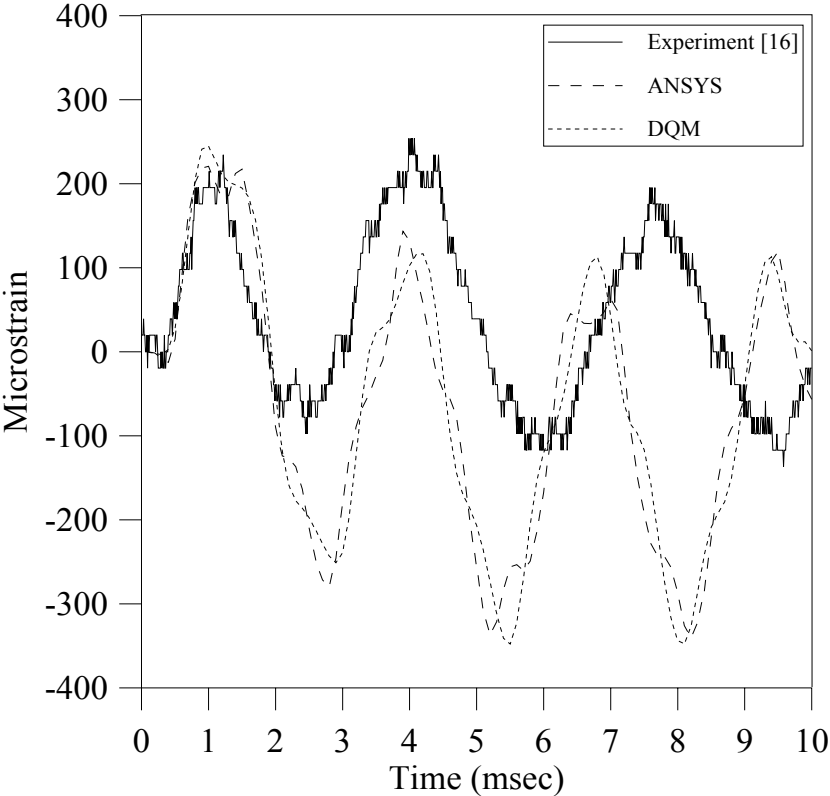
Figure 6.3: Displacement-time history of plate centre for the blast-loaded simply supported aluminium plate (M1) of Constant Thickness.
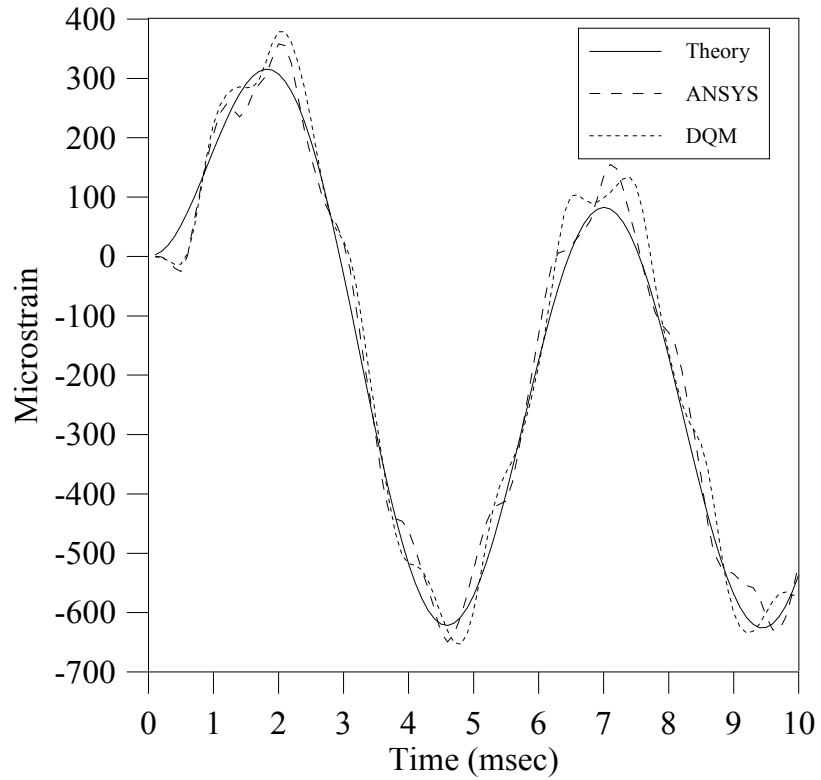

Figure 6.4: Strain-time history of plate centre for the blast-loaded simply supported aluminium plate (M1) of Constant Thickness.

43

The strain-time history result of the steel plate (M2) of constant thickness is shown in Figure 6.5 for the clamped plate and in Figure 6.6 for the simply supported plate. A better agreement is found between the experimental and predicted results for the steel plate (M2). This is because of that the unused nonlinear terms are not very effective on the solution and so the response of the steel plate seems to be still in the linear range [20].
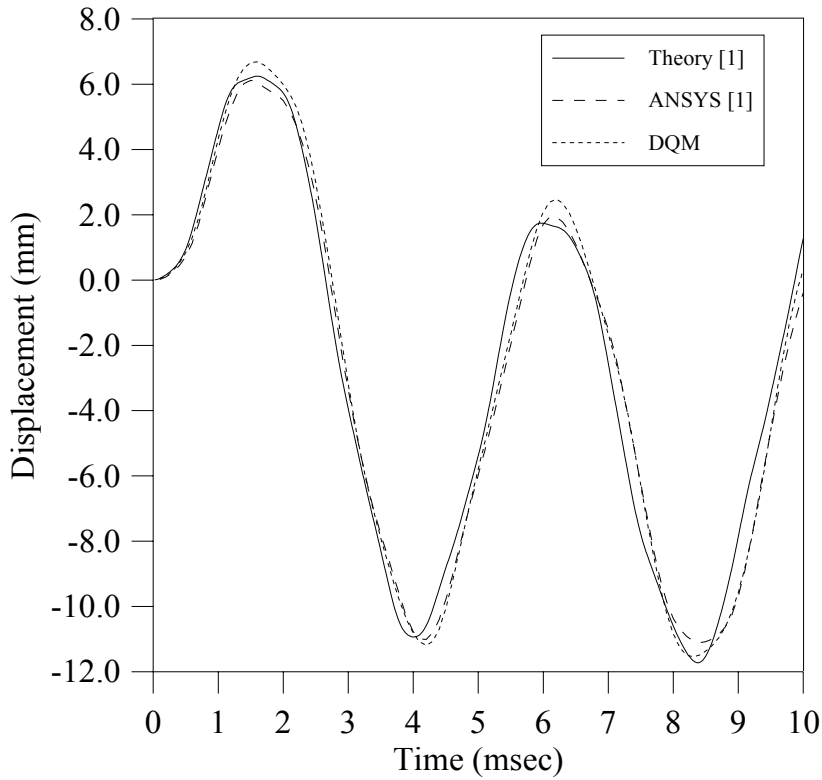

Figure 6.5: Strain-time history of plate centre for the blast-loaded clamped steel plate (M2) of constant thickness.
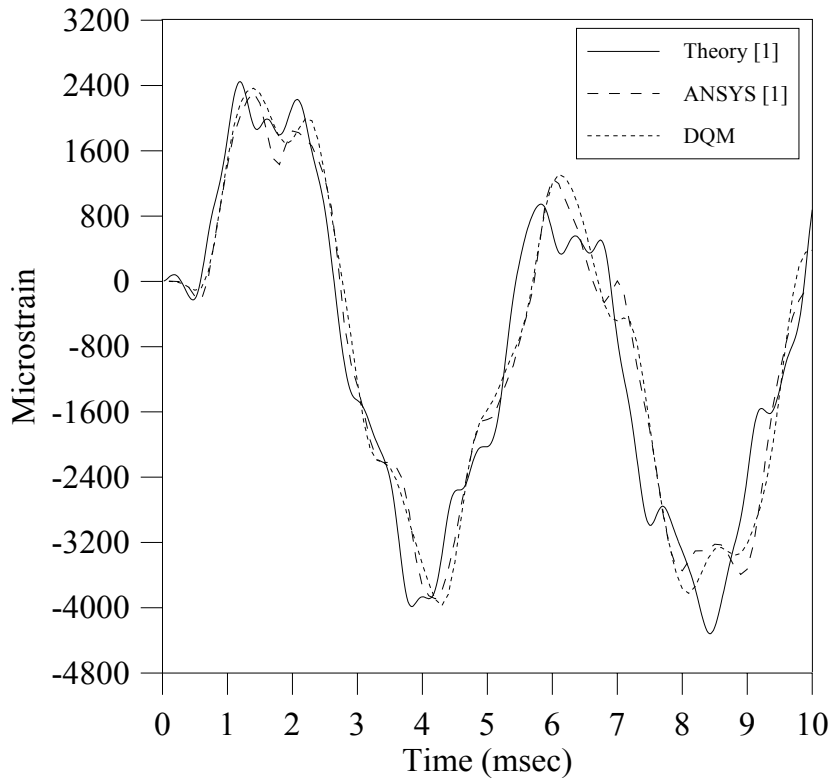
Figure 6.6: Strain-time history of plate centre for the blast-loaded
simply supported steel plate (M2) of constant thickness.

Figure 6.7 and Figure 6.8 show the displacement-time and strain-time histories of the centre of bidirectional laminated composite clamped plate (M3) of constant thickness, respectively. The results indicate that a better agreement between the predictions obtained using ANSYS and DQM is obtained compared to theoretical result.
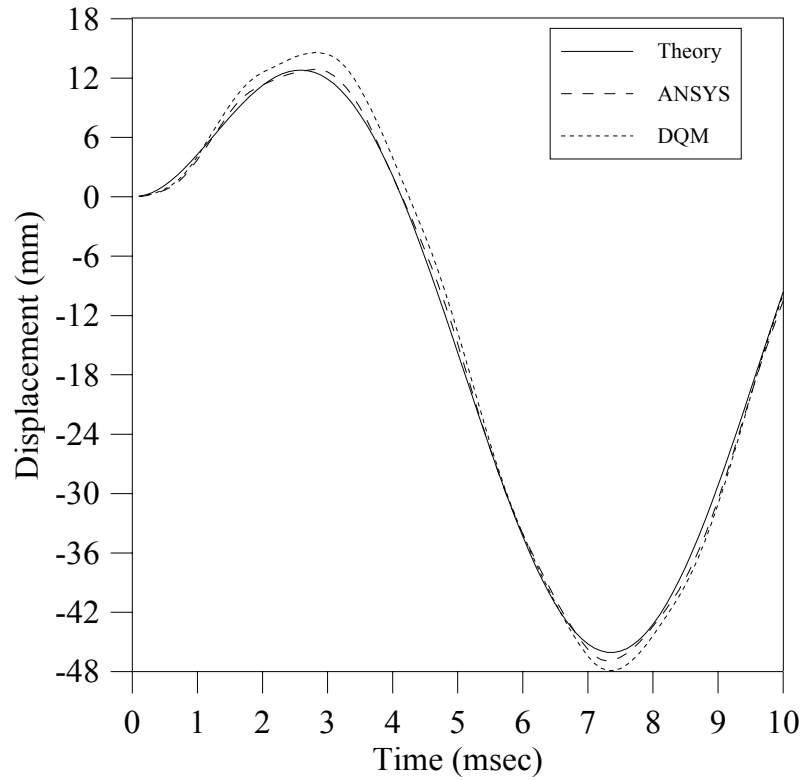
45

Figure 6.7: Displacement-time history of plate centre for the blast-loaded bidirectional laminated composite plate (M3) of constant thickness with clamped boundary condition.
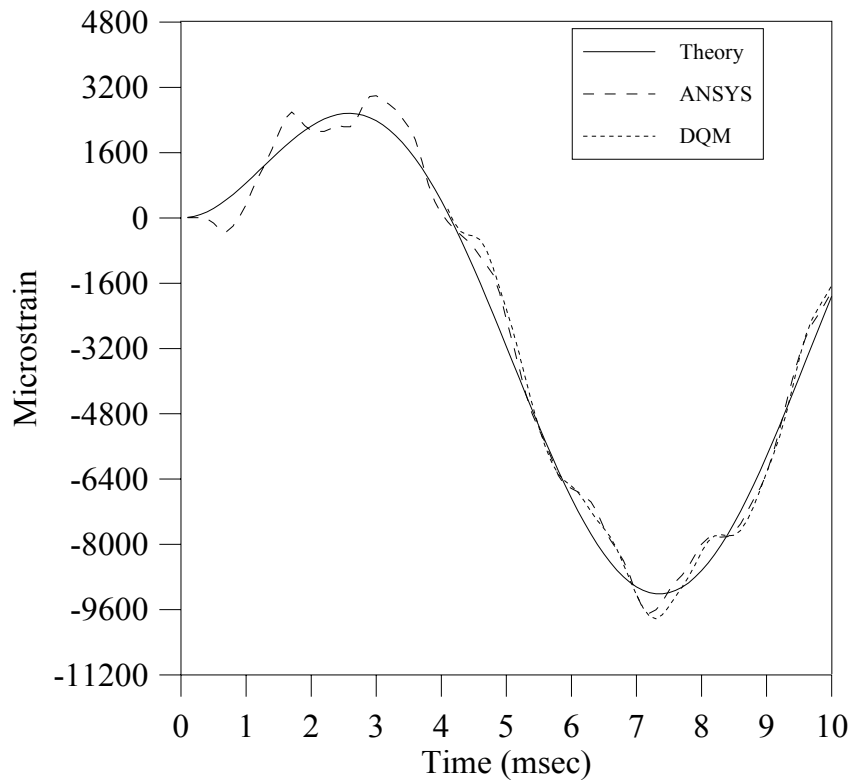

Figure 6.8: Strain-time history of plate centre for the blast-loaded bidirectional laminated composite plate (M3) of constant thickness with clamped boundary condition.

Figure 6.9 and Figure 6.10 show the displacement-time and strain-time histories of bidirectional laminated composite plate (M3) of constant thickness with simply supported boundary condition, respectively. The results again indicate an agreement between the predictions obtained using DQM, ANSYS and theory.
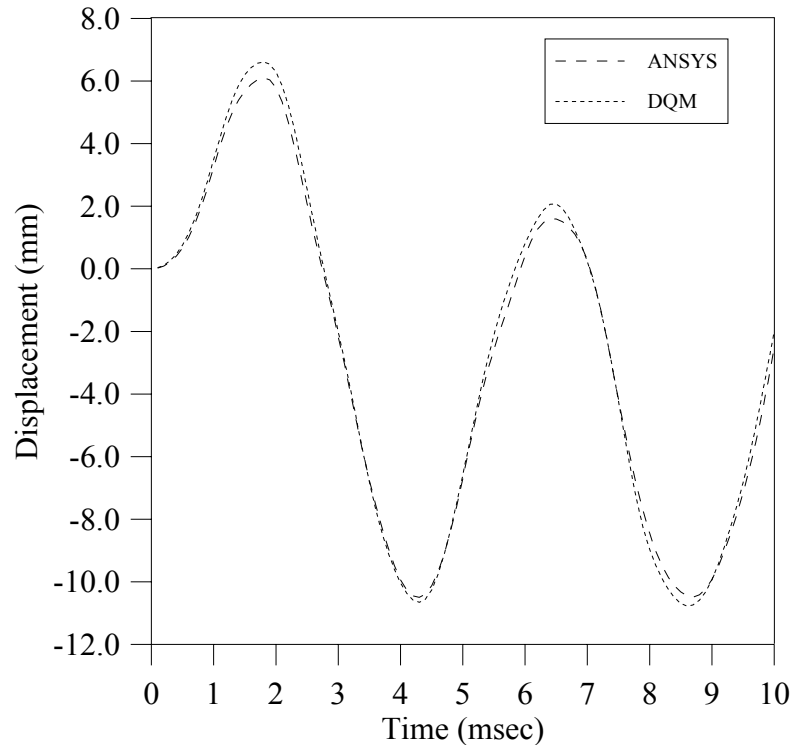

Figure 6.9: Displacement-time history of plate centre for the blast-loaded bidirectional laminated composite plate (M3) of constant thickness with simply supported boundary condition.
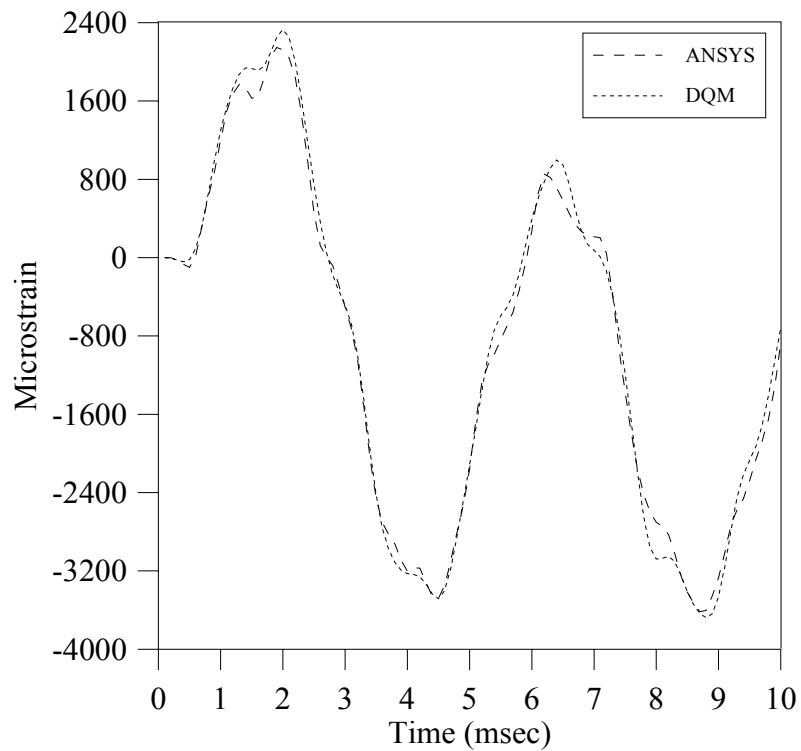
Figure 6.10: Strain-time history of plate centre for the blast-loaded bidirectional laminated composite plate (M3) of constant thickness with simply supported boundary condition.

Figure 6.11 and Figure 6.12 show the displacement-time and strain-time histories of unidirectional laminated composite plate (M4) of constant thickness with clamped boundary condition, respectively. For the mentioned plate configuration only DQM and ANSYS results are compared in the graphs. It can be concluded from these graphs that DQM presents very close solutions compared to ANSYS.
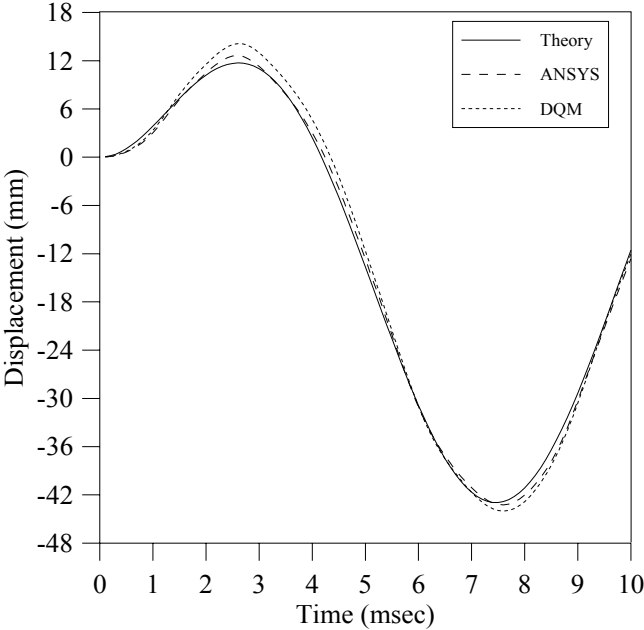
Figure 6.11: Displacement-time history of plate centre for the blast-loaded unidirectional laminated composite plate (M4) of constant thickness with clamped boundary condition.

Figure 6.12: Strain-time history of plate centre for the blast-loaded unidirectional laminated composite plate (M4) of constant thickness with clamped boundary condition.
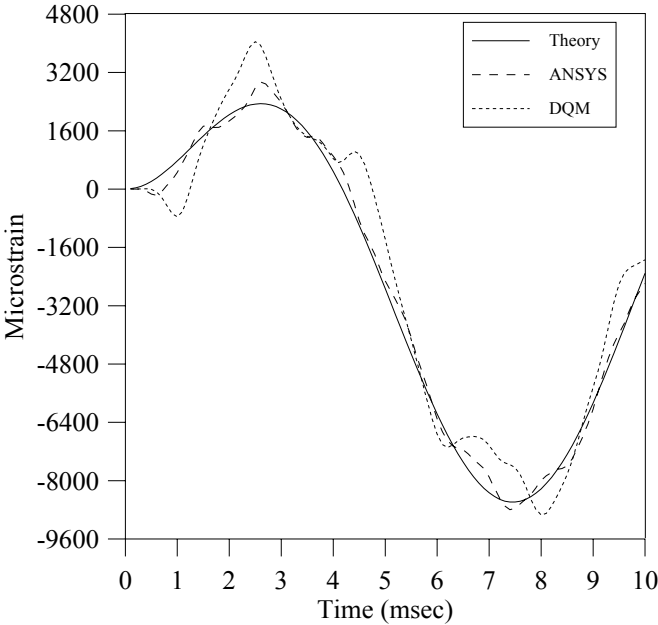
Figure 6.13 and Figure 6.14 show the displacement-time and strain-time histories of unidirectional laminated composite plate (M4) of constant thickness with simply supported boundary condition, respectively. A good agreement between the results of DQM and ANSYS is observed from the figures.

Figure 6.13: Displacement-time history of plate centre for the blast-loaded unidirectional laminated composite plate (M4) of constant thickness with simply supported boundary condition.

Figure 6.14: Strain-time history of plate centre for the blast-loaded unidirectional laminated composite plate (M4) of constant thickness with simply supported boundary condition.

Figure 6.15 and Figure 6.16 show the displacement-time and strain-time histories of unidirectional laminated composite plate (M5) of constant thickness with clamped boundary condition, respectively. A good agreement between the results of DQM and ANSYS is observed from the figures.
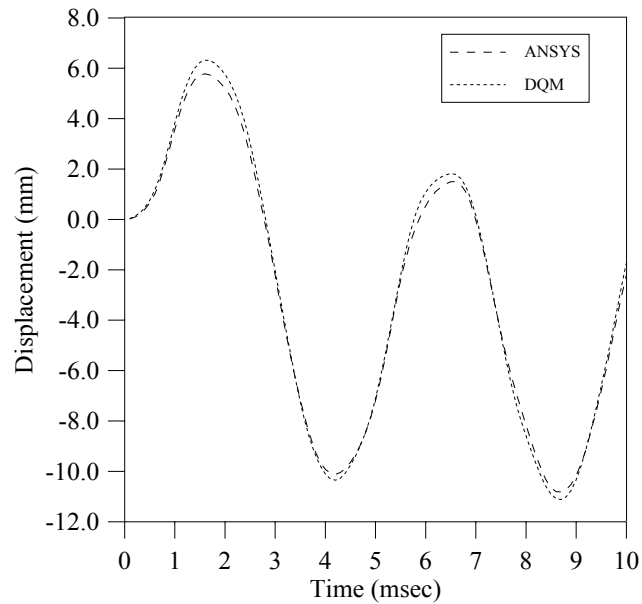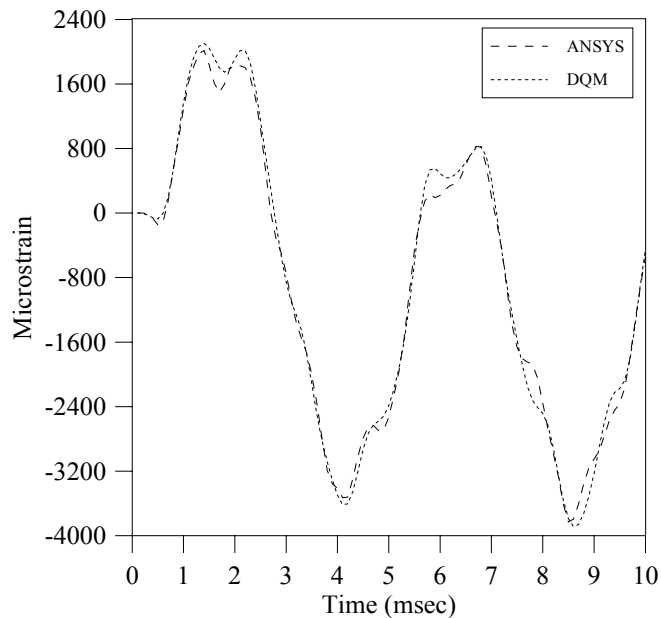

Figure 6.15: Displacement-time history of plate centre for the blast-loaded unidirectional laminated composite plate (M5) of constant thickness with clamped boundary condition.

Figure 6.16: Strain-time history of plate centre for the blast-loaded unidirectional laminated composite plate (M5) of constant thickness with clamped boundary condition.

Figure 6.17 and Figure 6.18 show the displacement-time and strain-time histories of unidirectional laminated composite plate (M5) of constant thickness with simply supported boundary condition, respectively. The results indicate an agreement between the predictions obtained using ANSYS and DQM. There is a discrepancy observed between the strain-time histories obtained by DQM and theory for the simply supported plates in the Figures 6.10, 6.14 and 6.18. However, a good agreement is obtained for the displacement-time histories of the mentioned plates using DQM and ANSYS. Furthermore, better solutions for both displacement-time and strain-time histories are obtained by DQM in compare with of ANSYS for the clamped plates.
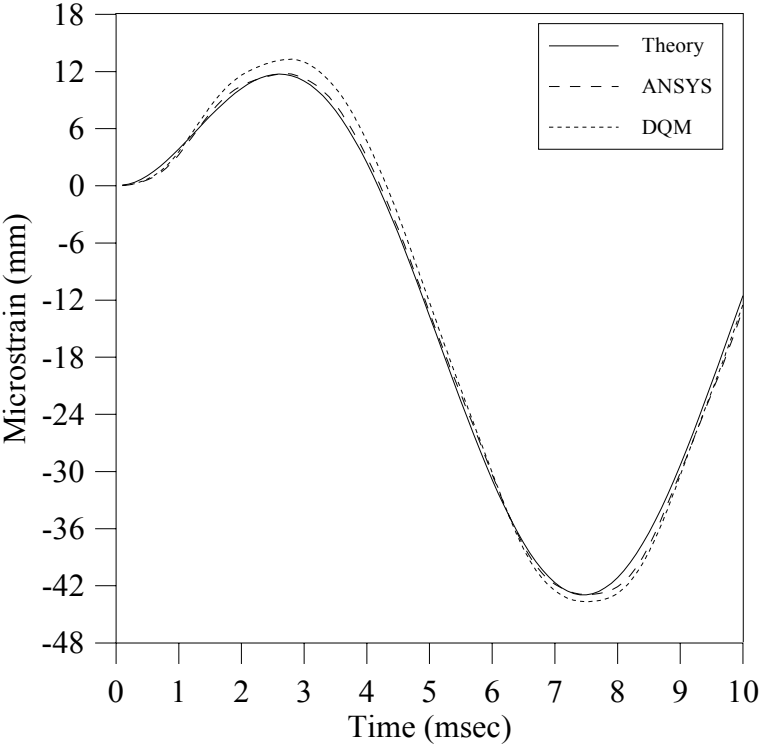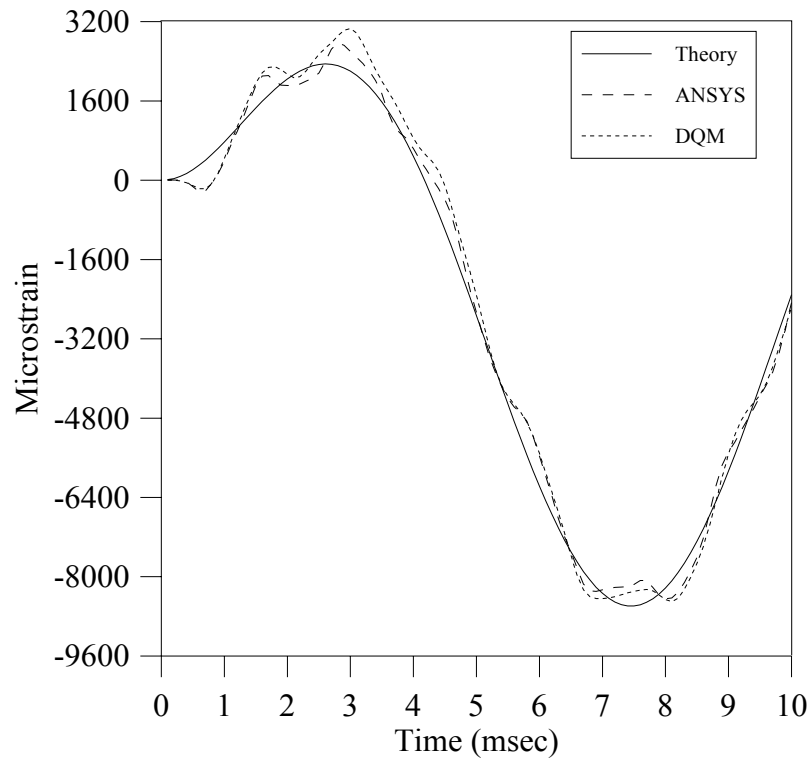

Figure 6.17: Displacement-time history of plate centre for the blast-loaded unidirectional laminated composite plate (M5) of constant thickness with simply supported boundary condition.

Figure 6.18: Strain-time history of plate centre for the blast-loaded unidirectional laminated composite plate (M5) of constant thickness with simply supported boundary condition.

It can also be concluded from the figures that the bidirectional laminated plate seems to be weaker against the blast loading in comparison to the unidirectional laminated plate. Also, the stacking sequence has an important effect on the plate response. The [0/90/0/90/0/90/0] stacking sequence is found to be more resistant to the blast loading compared to the $[0]_7$. Lastly, it is observed from the figures that the structural behaviour of plates obtained by DQM is less stiff than obtained by ANSYS at most plate configuration.

6.2 Numerical Results for The Plates of Variable Thickness

In this section, numerical results for the tapered plates that obtained using DQM are presented and compared to ANSYS results. The governing DQM equations for tapered plates have been derived earlier for the each analysis in the Sections 3.3, 3.4, 4.3, 4.4, 5.3 and 5.4.

Two types of materials, one isotropic and one laminated composite material, are considered for the analyses of tapered plates. The properties of the used isotropic

material, aluminium (M1), are given in the Table 6.1. The taper ratio is assumed to be 0.7, $\beta = 0.7$, and the aspect ratio is assumed to be 1, $\lambda = 1$, for the isotropic plate. Shell 63 element is used in modelling of the isotropic tapered plate in ANSYS. The finite element model of the isotropic tapered plate is represented in Figure 6.19. Moreover, cross section of the regarding plate is also shown in Figure 6.20 which illustrates the tapering along the *x*-axis.
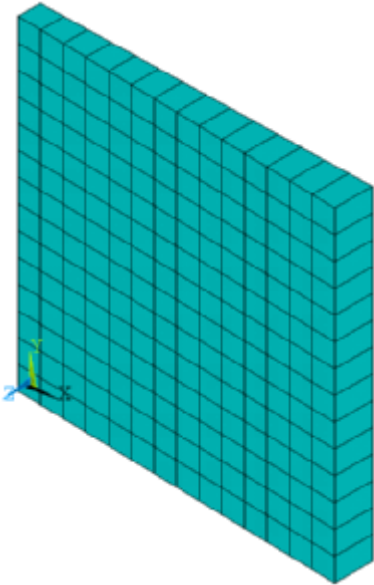
Figure 6.19: Finite element model of the isotropic tapered plate
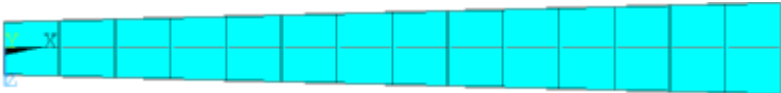
Figure 6.20: Cross section of the isotropic tapered plate.

In the Table 6.2, properties of the used laminated composite material (M3) are given. As told in the sections of analysis an approach was followed that takes the possible production method of such tapered laminated composite plate into consideration. That is to say, the plate is assumed to be 2-layered at the thinnest edge, at *X*=0, and 14-layered at the thickest edge, at *X*=1. Tapering has been increased from 2 layers to 14 layers by using 2 more layers at each 2 elements (considering 15 grid points and 14 elements) along the *x*-axis. However, it should be expressed that at the points

where the number of layers increase, the average of number of layers is taken as the number of layers in order to obtain better approximation in DQM solutions. In other words, at intersection points where extra layers are added the number of layers is assumed to be average of old and new number of layers along x-axis. For instance, at grid point 3 of Figure 6.22 the number of layer is assumed to be 3 whereas it is assumed to be 5 layers at grid point 5. Following this manner the plate is assumed to have 13 layers at grid point 13 and 14 layers at points 14 and 15. Experience shows that the mentioned assumption related to the number of layers at intersection grid points provides solutions with better accuracy in DQM analysis.

The ply orientation angle is assumed to be 0° for each layer for the mentioned composite plate. The finite element model of laminated composite tapered plate is represented in Figure 6.21. Moreover, cross section of the regarding plate is also shown in Figure 6.22 which illustrates the tapering 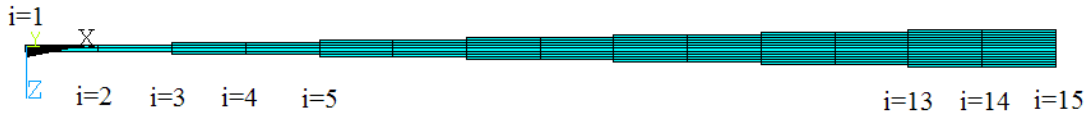along the x-axis. As was in the modelling of isotropic plate, Shell 63 element is used to model the laminated tapered composite plate.
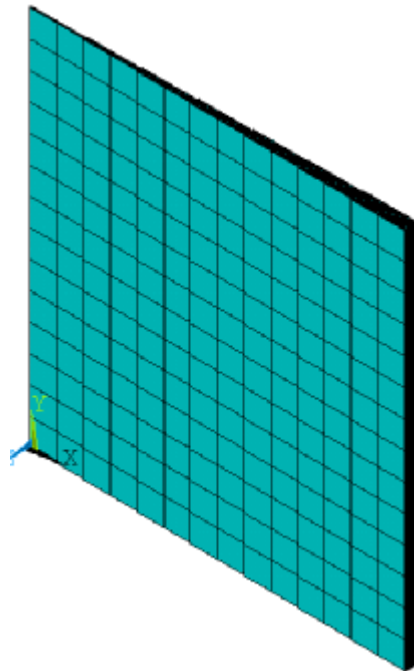
Figure 6.21: Finite element model of the laminated composite tapered plate.

Figure 6.22: Cross section of the laminated composite tapered plate.

The dimensional centre deflections of the isotropic and laminated composite tapered plates are given in Table 6.9 for the simply supported and clamped boundary conditions. From the results given in the Table 6.9 it can be concluded that DQM provides better solutions for clamped boundary condition than simply supported for isotropic and composite tapered plates. The difference between the deflection results of DQM and ANSYS is more than 20 percent for simply supported and clamped tapered plates of (M1). A similar difference between the deflections obtained using DQM and ANSYS is obtained for the simply supported tapered plate of (M3) which is nearly 20 percent. However, the discrepancy between the DQM and ANSYS results is less than 8 percent for the clamped tapered composite plate of (M3). In these analyses, the distributed load is taken 2890.6 N/m^2 for the plates of (M3) and 28906 N/m^2 for the plates of (M1).

Table 6.9: The dimensional centre deflections (mm), *w*, of the square plates of variable thickness.

	(S-S-S-S)		(C-C-C-C)	
	DQM	ANSYS	DQM	ANSYS
M1	7.006	5.224	2.190	1.655
M3	3.099	2.465	0. 626	0.583

In Table 6.10, the dimensional free vibration frequencies are given for the first ten modes for the simply supported and clamped tapered isotropic plate, (M1). As can be noted, better agreement is obtained for the simply supported isotropic tapered plate. In Table 11, however, the dimensional free vibration frequencies are given for the first ten modes for the simply supported and clamped tapered laminated composite plate, (M3). The fundamental frequencies obtained by DQM for the laminated composite tapered plate have approximately 5 percent difference for the simply supported and 10 percent for the clamped plate compared to the ANSYS results.

Table 6.10: The dimensional frequencies (Hz), ω, of the isotropic (M1) square plate of variable thickness for the first ten modes.

| Mode	C-C-C-C		S-S-S-S	
	DQM	ANSYS	DQM	ANSYS
1	363.49	362.31	200.89	200.63
2	736.57	732.84	496.98	495.79
3	741.55	737.87	500.23	498.95
4	1096.70	1086.3	802.27	797.86
5	1306.52	1297.6	977.86	974.28
6	1331.52	1323.5	998.22	994.72
7	1668.57	1648.0	1299.57	1289.3
8	1678.48	1658.1	1307.45	1297.5
9	1758.25	2033.4	1632.18	1623.5
10	2051.57	2109.3	1695.17	1687.8

Table 6.11: The dimensional frequencies (Hz), ω, of the laminated composite (M3) square plates of variable thickness for the first ten modes.

| Mode	C-C-C-C		S-S-S-S	
	DQM	ANSYS	DQM	ANSYS
1	237.77	211.94	115.64	109.02
2	458.83	389.75	285.39	262.98
3	495.41	424.33	313.38	272.89
4	693.98	611.52	475.24	448.44
5	726.71	626.13	543.58	449.01
6	785.41	750.46	648.58	560.67
7	821.02	869.48	780.65	668.86
8	894.72	924.72	784.39	702.43
9	1039.94	946.45	863.99	743.22
10	1064.46	1163.7	1094.80	921.20

Two types of strain-time histories are obtained for the each tapered plate since the strains ε_X and ε_Y are not equal due to the variation of plate thickness along one direction. Both ε_X- and ε_Y-time histories are given here for the isotropic (M1) tapered plate. On the other hand, ε_Y-time history is given only for the laminated composite (M3) tapered plate since the significant divergence of ε_X-time graphs obtained using DQM compared to ANSYS. Although DQM provides a reasonable convergence for both strains ε_X and ε_Y in both direction for the isotropic tapered plates, the ε_X-time histories, that computed along the x-direction where the tapering exists, for the composite plates did not converge to the ANSYS results. These graphs are not given here due to this reason. However, various researches are still carried on

in order to clarify the reason of the mentioned discrepancy of the strain-time history along the tapering direction of composite plates.
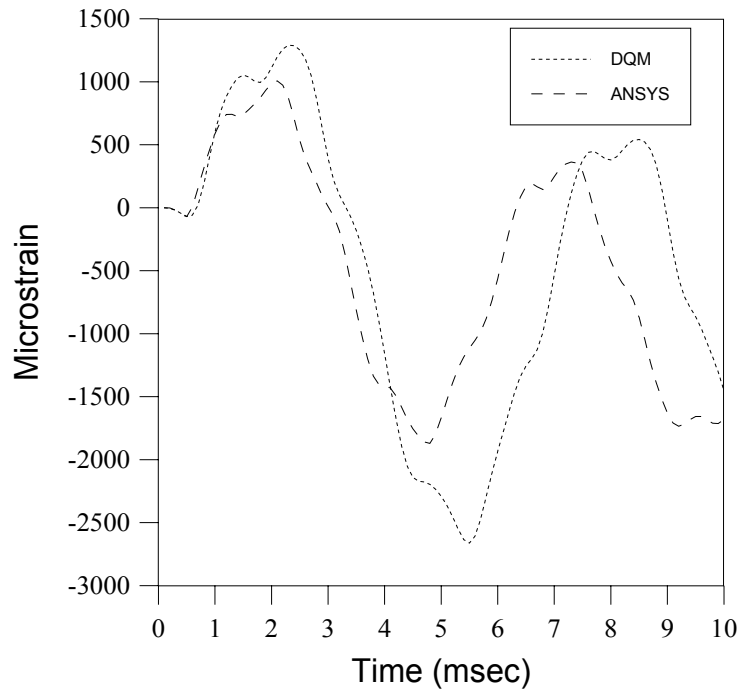
Figure 6.23, Figure 6.24 and Figure 6.25 show the displacement-time and strain-time histories of the simply supported tapered aluminium plate (M1), respectively. As can be noted, Figure 6.24 represents the strain-time history of center of tapered isotropic plate along the x-direction whereas Figure 6.25 represents the strain-time history of center of tapered isotropic plate along the y-direction. A reasonable convergence is obtained in each graph using DQM compared to ANSYS for the simply supported plate. The blast load parameter is taken as p_m=28906.0 N/m^2 in the analyses of isotropic (M1) tapered plates.
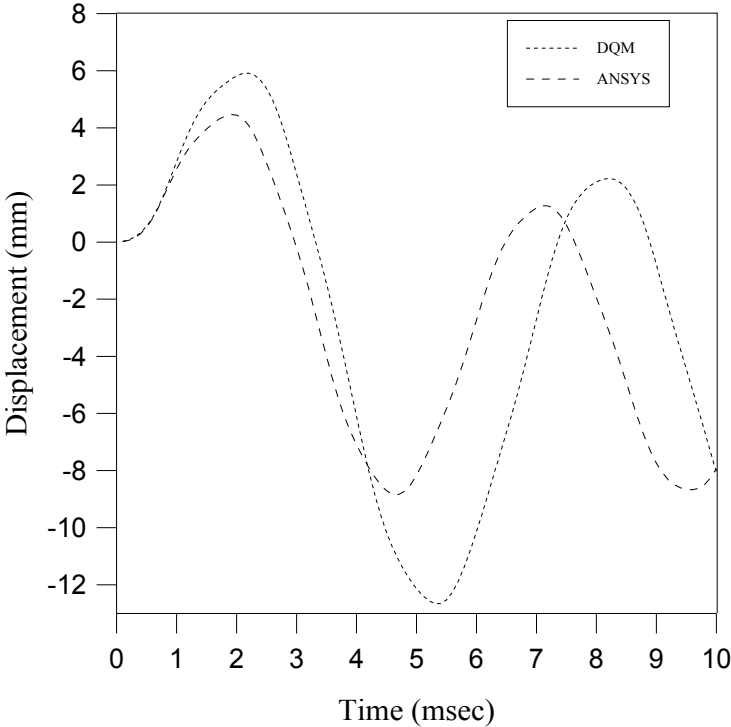
Figure 6.23: Displacement-time history of plate centre for the blast-loaded
isotropic plate (M1) of variable thickness with
simply supported boundary condition.
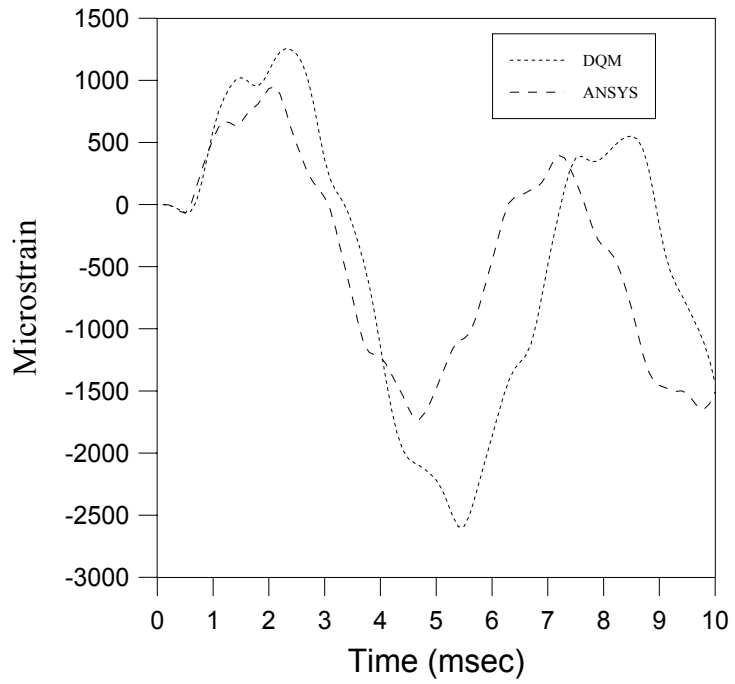
Figure 6.24: Strain-time (ε_X) history of plate centre for the blast-loaded isotropic plate (M1) of variable thickness with simply supported boundary condition.

Figure 6.25: Strain-time (ε_Y) history of plate centre for the blast-loaded isotropic plate (M1) of variable thickness with simply supported boundary condition.

Figure 6.26 show the displacement-time history of blast loaded clamped isotropic (M1) tapered plate. Figure 6.27 and 6.28 show the strain-time histories for ε_X and ε_Y of the clamped tapered aluminium (M1) plate, respectively. Again a reasonable convergence is obtained in each graph using DQM compared to ANSYS for the clamped tapered isotropic plate. However the discrepancy between the DQM and ANSYS results is more apparent for the clamped tapered plate than the simply supported one since there are more peaks in displacement- and strain-time graphs of clamped plate as can be seen in Figure 6.26, 6.27 and 6.28.

Figure 6.26: Displacement-time history of plate centre for the blast-loaded
                isotropic plate (M1) of variable thickness with
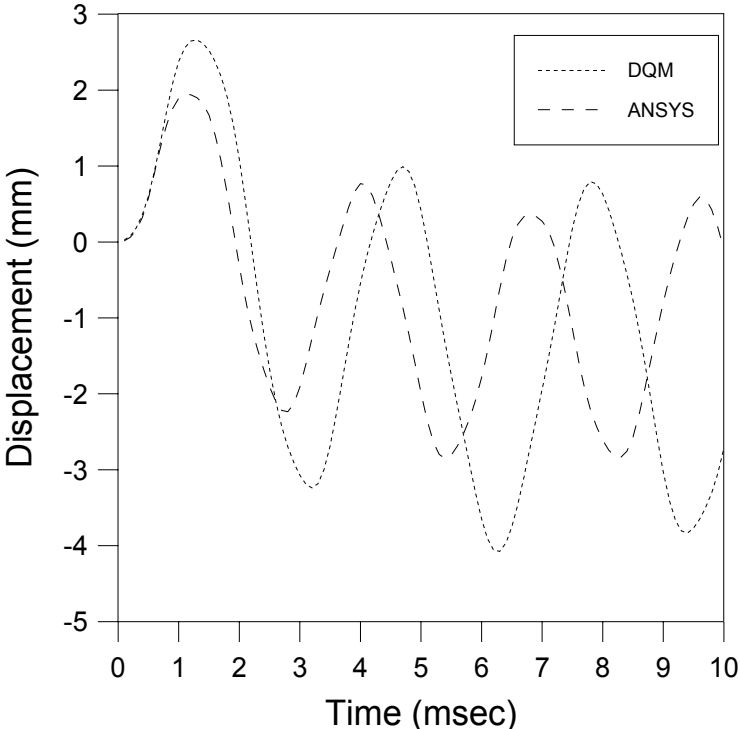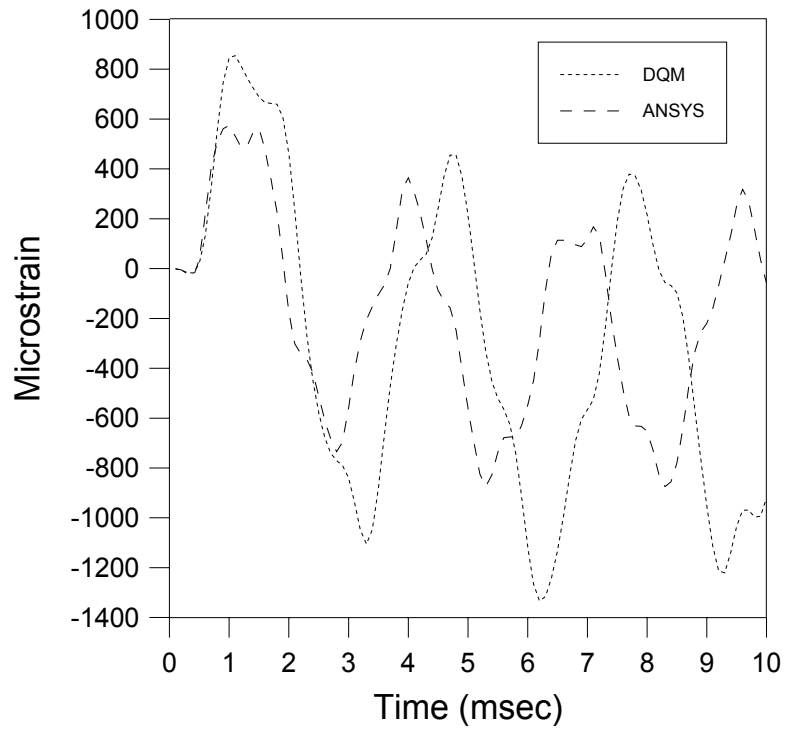   clamped boundary condition.

Figure 6.27: Strain-time (ε_X) history of plate centre for the blast-loaded isotropic plate (M1) of variable thickness with clamped boundary condition.

Figure 6.28: Strain-time (ε_Y) history of plate centre for the blast-loaded isotropic plate (M1) of variable thickness with clamped boundary condition.

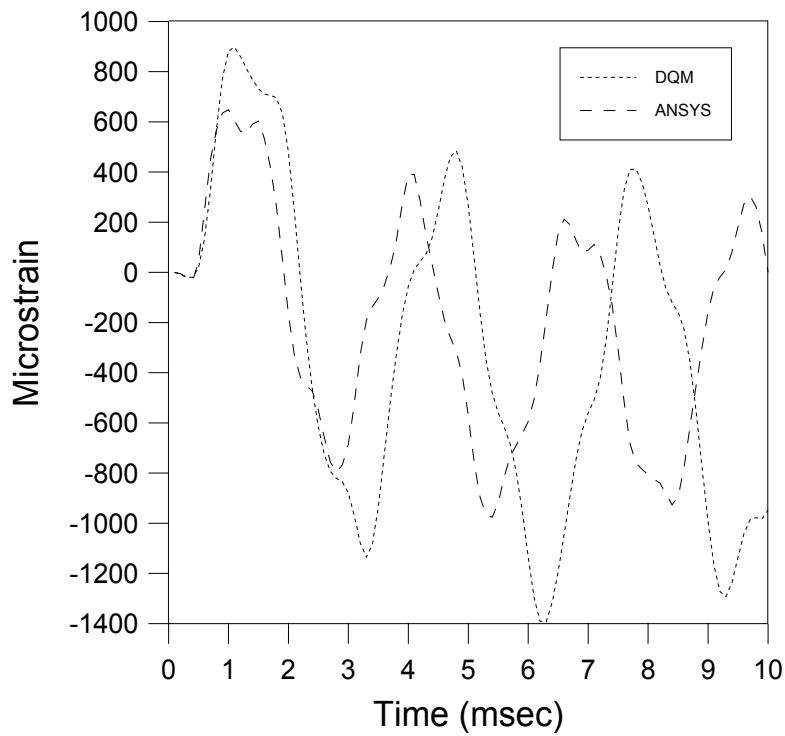In Figure 6.29 and 6.30, the displacement-time and strain-time (ε_Y) histories are given for the tapered laminated composite plate (M3) with simply supported boundary condition.
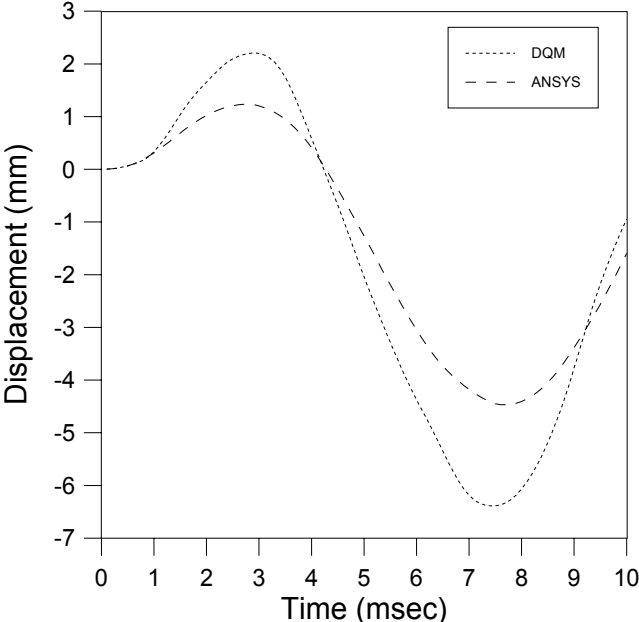
Figure 6.29: Displacement-time history of plate centre for the blast-loaded bidirectional laminated composite plate (M3) of variable thickness with simply supported boundary condition.
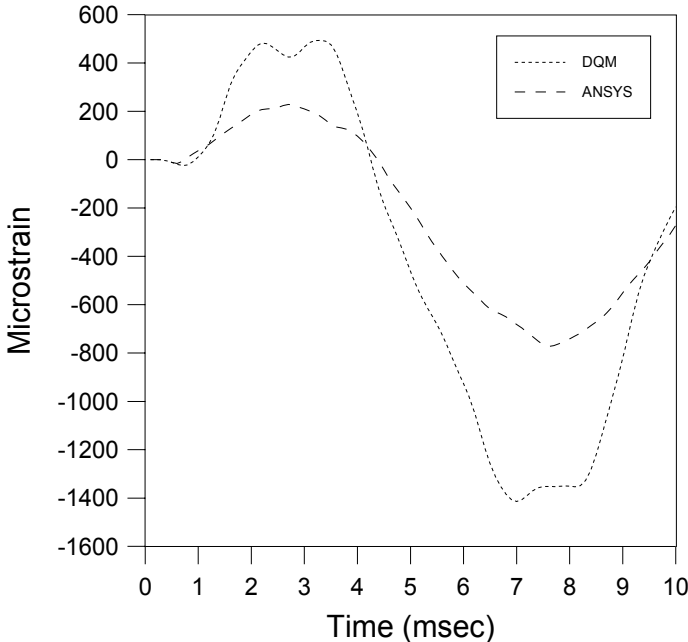
Figure 6.30: Strain-time (ε_Y) history of plate centre for the blast-loaded bidirectional laminated composite plate (M3) of variable thickness with simply supported boundary condition.

In Figure 6.31 and 6.32, the displacement-time and strain-time (ε_Y) histories are given for the tapered laminated composite plate (M3) with clamped boundary condition.

Figure 6.31: Displacement-time history of plate centre for the blast-loaded bidirectional laminated composite plate (M3) of variable thickness with clamped boundary condition.

Figure 6.32: Strain-time (ε_Y) history of plate centre for the blast-loaded bidirectional laminated composite plate (M3) of variable thickness with clamped boundary condition.
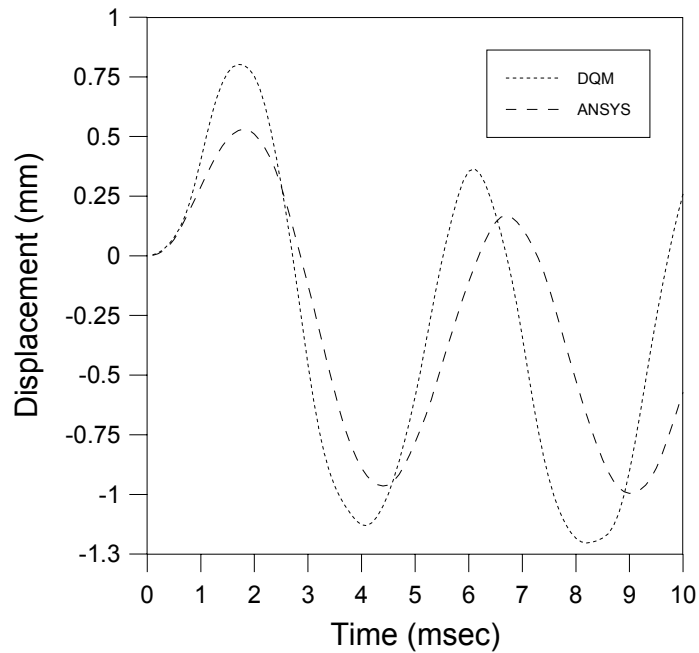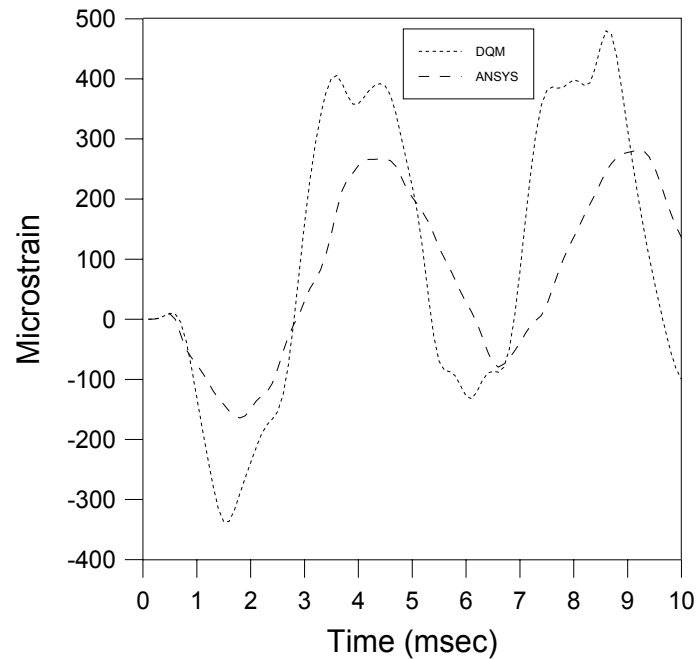
In the analyses of tapered laminated composite (M3) plates the blast load parameter is taken as $p_m = 2890.6 \ N/m^2$. It can be concluded from the Figures 6.29 to 6.32 that the DQM do not exhibit a good convergence for the displacement- and strain-time (ε_Y) histories for the (M3) tapered laminated tapered plate although an approximation to ANSYS results is obtained. Even, the strain-time (ε_X) histories for the mentioned plate obtained using DQM is quite erratic in comparison with ANSYS which is why these graphs were left out in the reported graphs of this work.

Generally, the results show that the DQM can be used for the prediction of transient responses of both isotropic and composite plates. Experience shows that the computer time is much lower with DQM compared to the computer time in the finite element solution. This could be an advantage of DQM when analyzing the long time transient response of plates. Although, some analyses need to be inspected on more, DQM gives also accurate results for the tapered isotropic and laminated composite plates. This means DQM can easily be utilized in analyzing of the complicating affects in plates such as thickness variation and material anisotropy.

7. CONCLUSION

Static, free vibration and transient analyses of various rectangular plates are accomplished by differential quadrature method (DQM) in the present thesis. Plates are analyzed from various aspects such as plate material and thickness. Various isotropic materials and laminated composite materials are taken into consideration. Two type of boundary conditions are considered for the regarding plates: Clamped and simply supported on all four edges. In the analyses of plates of variable thickness, the variation in the thickness is assumed to be just along the *x*-axis.

In the first section of the present study, contents of the present study are presented together with a brief literature survey for the DQM. In the second section, DQM is described from the mathematical aspect, and some assumptions and approaches about DQM are expressed. The sections 3, 4 and 5 are all divided to four sub-parts which analyze, respectively, isotropic and composite plates of constant thickness and variable thickness. In Section 3, deflection analysis; in Section 4 free vibration analysis and in Section 5 transient analysis are achieved for the mentioned plates using DQM. In the section of transient analysis, all plates are assumed to be exposed to blast loading and the resulting equations are solved by the Newmark numerical time integration method. Furthermore, FORTRAN programs were developed in order to solve the DQM governing analog equations in each section.

In section 6, the numerical results are presented together with the used material properties. The numerical results are presented in two sub-sections, namely, numerical results for plates of constant and variable thickness. In both sub-sections the center deflections of isotropic and laminated composite plates are given firstly. Further, the free vibration frequencies of each plate configuration are presented. While the frequencies and deflections of plates of constant thickness are given as dimensionless, they are given dimensional for the plates of variable thickness for convenience. To see the accuracy of obtained results, the DQM results are mainly compared to ANSYS software results; however, some available theoretical and literature results are also employed in the comparisons.

After the accuracy of DQM solutions is verified by comparing the deflection and frequency of the regarding plate configurations with ANSYS results the DQM solutions are extended to solve the equations that governs structural behaviour of plates subjected air blast load. Displacement- and strain-time histories are obtained for each plate configuration and compared mainly to ANSYS results and also for some plate configurations theoretical and experimental results are employed in the comparisons.

Very accurate results are obtained by DQM for the plates of constant thickness. The center deflections and fundamental frequencies of each plate configuration of constant thickness are obtained very close to ANSYS results. Furthermore, displacement- and strain-time histories obtained using DQM for the plates of constant thickness are found to be in a good agreement with ANSYS. However, a discrepancy was observed between the strain-time histories of DQM and experimental data for the fully clamped aluminium and steel plates. This discrepancy can be attributed to the effect of nonlinear terms that are unused in the analyses.

The results obtained using DQM for the plates of variable thickness did not converge very well for each plate configuration. For instance, there are approximately 30 percent differences between the center deflections obtained by DQM and ANSYS for the isotropic tapered C-C-C-C and S-S-S-S plates although the fundamental frequencies of mentioned plates are estimated very well. On the other hand, the displacement- and strain-time (ε_X, ε_Y) histories of isotropic tapered plates obtained using DQM exhibit reasonable convergence compared to ANSYS results. However, this is not the case for the tapered laminated composite plate. There are considerable differences observed in the strain-time (ε_Y) histories of the mentioned plates. As mentioned in the previous section ε_X-time histories for the tapered laminated composite plates were left out in the reported results of this work since the divergence obtained was very significant. However, more reasonable results were obtained in the static and free vibrational analyses of these plates.

In general, DQM provides solutions with acceptable accuracy in the analyses of plates. Also, the results obtained in the static and free vibrational analyses of plates are very accurate compared to ANSYS and other available results from the literature. Furthermore, the results show that the DQM can be used for the prediction of

transient responses of both isotropic and composite plates. The computer time is much lower with DQM compared to the computer time in the finite element solution. Although, some analyses need to be inspected on more, DQM gives also accurate results for the tapered isotropic and composite plates. This means DQM can be implemented in analyzing of the complicating affects in plates such as thickness variation and material anisotropy, straightforwardly. As was stated by Bert and Malik [10], DQM has the capability of producing highly accurate solutions with minimal computational effort at some type of engineering problems, and therefore, has the potential of being an alternative to the conventional techniques such as the finite difference and finite element methods in the future. Therefore, in the future studies, it is intended to involve the various nonlinear affects in the DQM analyses of plates and also it is considered to implement the semi-analytical DQM solution into the transient analyses of plates.

REFERENCES

[1] **Turkmen, H.S. and Mecitoğlu, Z.**, 1999, "Nonlinear structural response of laminated composite plates subjected to blast loading.", *AIAA Journal*, Vol. 37, N. 12, pp. 1639-1647.

[2] **Bellman, R.E. and Casti, J.**, 1971, "Differential quadrature and long term integration.", *Journal of Mathematical Analysis and Applications*, Vol. 34, pp. 235-238.

[3] **Bellman, R., Kashef, B.G. and Casti, J.**, 1972, "Differential quadrature: a technique for the rapid solution of nonlinear partial differential equations.", *J. Comput. Phys*. Vol. 10, pp. 40-52.

[4] **Civan, F. and Sliepcevich, C.M.**, 1983, "Application of differential quadrature to transport process.", *Journal of Math. Analy. Appl.*, Vol. 93, pp. 206-221.

[5] **Civan, F. and Sliepcevich, C.M.**, 1984, "Differential quadrature for multidimensional problems.", *Journal of Math. Analy. Appl.*, Vol. 101, pp. 423-443.

[6] **Mingle, J.O.**, 1984, "The method of differential quadrature for transient nonlinear diffusion.", *Journal of Math. Analy. Appl.*, Vol. 60, pp. 559-569.

[7] **Bert, C.W., Jang, S.K., and Striz, A.G.**, 1988, "Two new approximate methods for analyzing free vibration of structural components.", *AIAA Journal*, Vol. 26, pp. 612-618.

[8] **Malik, M. and Bert, C.W.**, 1996, "Implementing multiple boundary conditions in the DQ solution of higher-order pde's: application to free vibration of plates.", *Int. Journal for Numerical Methods in Engineering*, Vol. 39, pp. 1237-1258.

[9] **Jang, S.K., Bert, C.W., and Striz, A.G.**, 1988, "Application of the differential quadrature to static analysis of structural components.", *Int. Journal for Numerical Methods in Engineering*, Vol. 28, pp. 561-577.

[10] **Bert, C.W. and Malik, M.**, 1996, "Differential quadrature method in computational mechanics: A Review.", *Appl. Mech. Rev.*, Vol. 49, pp. 1-28.

[11] **Du, H., Lim, M.K., and Lin, N.R.**, 1994, "Application of generalized differential quadrature method to structural problems.", *Int. J. Num. Meth. Eng.*, Vol. 37 pp. 1881-1896.

[12] **Wang, X, Bert, C.W., and Striz, A.G.**, 1993, "Differential quadrature analysis of deflection, buckling, and free vibration of beams and rectangular plates.", *Computers and Structures* Vol. 48(3), pp. 473-479.

[13] **Shu, C. and Richards, B.E.**, 1992, "Application of generalized differential quadrature to solve two-dimensional incompressible Navier-Stokes equations," *Int. J. Num. Meth. Fluids*, Vol. 15, pp. 791-798.

[14] **Leissa, A.W.**, 1973, "The free vibration of rectangular plates," *J. Sound Vib.*, Vol. 108, pp. 257-293.

[15] **Bert, C.W., Malik M.**, 1997, "Differential quadrature: a powerful new technique for analysis of composite structures.", *Composite Structures*, Vol. 39, Nos 3-4, pp. 179-189.

[16] **Turkmen, H.S.**, 1998, "Structural response of isotropic plates subjected to blast loading.", *Advances in Computational Structural Mechanics*, Edinburgh, Scotland, pp. 101-107.

[17] **Kukreti, A.R., Farsa, J. and Bert, C.W.**, 1992, "Fundamental frequency analysis of tapered plates by differential quadrature.", *J. Engrg. Mech.*, Vol. 118, pp 1221-1238.

[18] **Farsa, J.**, "Development of a differential quadrature technique for the fundamental frequency analysis of tapered, orthotropic, anisotropic and laminated thin plates.", 1991, *PhD Thesis* submitted to The University of Oklahoma, USA.

[19] **Farsa, J., Kukreti, A.R., and Bert, C.W.**, 1992, "Fundamental frequency analysis of single specially orthotropic, generally orthotropic and anisotropic rectangular layered plates by the differential quadrature method.", *Computers and Structures.*, Vol. 46, pp 465-477.

[20] **Tuna, M., Turkmen H.S.**, "Dynamic behaviour of a plate under air blast load using differential quadrature method.", *2007 ASME International Mechanical Engineering Congress and Exposition*, November 11-15, 2007, Seattle, Washington, USA, Paper IMECE2007-41553.

[21] **Tuna, M., Turkmen H.S.**, Anlık basınç yükü altındaki basit mesnetli plakların dinamik davranışının diferansiyel kareleme yöntemi ile incelenmesi., *XV. Ulusal Mekanik Kongresi*, 03-07 Eylül 2007, Isparta, Türkiye.

[22] **Bert, C.W., Wang, X., Striz, A.G.**, 1994, "Static and free vibrational analysis of beams and plates by differential quadrature method", *Acta Mechanica*, Vol. 102, pp. 11-24.

[23] **Bert, C.W., Wang, X., Striz, A.G.**, 1993, "Differential quadrature for static and free vibration analyses of anisotropic plates.", *Int. J. Solids Structures*, Vol. 30, No. 13, pp. 1737-1744.

[24] **Bert, C.W., Malik M.**, 1996, "The differential quadrature method for irregular domains and application to plate vibration.", *Int. J. Mech. Sci.*, Vol. 38, No. 6, pp. 589-606.

[25] **Bert, C.W., Malik M.**, 1996, "Free vibration analysis of tapered rectangular plates by differential quadrature method: A semi-analytical approach.", *J. Sound and Vibration*, Vol. 190(1), pp. 41-63.

[26] **Bert, C.W., Malik M.**, 1996, "Semianalytical differential quadrature solution for free vibration analysis of rectangular plates.", *AIAA Journal*, Vol. 34, No. 3, pp. 601-606.

[27] **Kazanci, Z., and Mecitoglu, Z.**, 2006, "Nonlinear damped vibrations of a laminated composite plate subjected to blast load," *AIAA Journal*, Vol. 44, No. 9, pp. 2002–2008.

[28] **Timoshenko, S.P. and Woinowsky-Krieger, S.**, 1959, "*Theory of Plates and Shells*", 2nd ed., McGraw-Hill, Singapore.

[29] **Ventsel, E., Krauthammer, T.**, 2001, *Thin Plates and Shells: Theory, Analysis, and Applications*, Marcel Dekker Inc., USA

[30] **Springer, G.S. and Kollar, L.P..**, 2003, "*Mechanics of Composite Structures*", 1st ed., Cambridge University Press, New York, USA.

CURRICULUM VITAE

Candidate's full name: Murat Tuna

Place and date of birth: Erzurum / 20.09.1983

Universities attended:

2009 – 2006 **MSc, Aeronautical Engineering, Istanbul Technical University**

2006 – 2001 **BSc, Aeronautical Engineering, Istanbul Technical University**

Publications:

- Tuna M, Türkmen H.S., "Dynamic behaviour of a plate under air blast load using differential quadrature method", *2007 ASME International Mechanical Engineering Congress and Exposition*, November 11-15, Seattle, Washington, USA

- Tuna M., Türkmen H.S., "Anlık basınç yükü altındaki basit mesnetli plakların dinamik davranışının diferansiyel kareleme yöntemi ile incelenmesi.", *XV. Ulusal Mekanik Kongresi*, 03-07 Eylül 2007, Isparta, Türkiye